PETROPHYSICS, VOL. 42, NO. 6 (NOVEMBER-DECEMBER 2001); P. 588–610; 8 FIGURES, 1 TABLE

Foundations of Tensor Induction Well-Logging

Michael Zhdanov[1], David Kennedy[2], and Ertan Peksen[1]

ABSTRACT

One of the most challenging problems in the field of electromagnetic well logging is the development of interpretation methods for the characterization of conductivity anisotropy in an earth formation. We examine the response of a triaxial electromagnetic induction well-logging instrument in an unbounded, homogeneous, transversely isotropic conductive medium. This instrument detects three components of magnetic field due to each of three transmitters for a total of nine signals. These can be mathematically organized as a tensor array which we call the magnetic induction tensor. The magnetic induction tensor components provide a general description of the electromagnetic field in a transversely isotropic medium. By theoretically analyzing the triaxial induction instrument for its response to the magnetic field components induced in the conductive medium, we derive low frequency approximations for the quadrature components of our induction tensor. Based on this analysis, we find that by measuring the quadrature components of the induction tensor in a deviated borehole, the conductivity anisotropy of the media can be resolved from the instrument response. This information includes not only the vertical and horizontal conductivities, but also the orientation of the logging instrument axis with respect to the tensor principal axes. We introduce the formulas for the apparent horizontal and vertical conductivities σ_{ha}, σ_{va}, the apparent anisotropy coefficient λ_a, and the apparent relative deviation angle α_a. These can be used as the basis for a tensor logging instrument response interpretation in unbounded, homogeneous, anisotropic media. The theory is illustrated by numerical examples of induction tensor calculations.

INTRODUCTION

Formation conductivity (or resistivity) determination from a well bore is probably the oldest geophysical technique to be applied in the subsurface and retains a preeminent place in logging suites today. Until recently resistivity logging instruments and interpretation techniques were considered mature and improvements in technique were evolutionary rather than revolutionary. This has been particularly true for the induction method. The emphasis in hardware improvements has been on the use of more axial dipole antennas on each instrument to better sample (or "sound") the radial conductivity distribution in order to better infer invasion profiles; i.e., the drilling-induced radial variation in conductivity. The use of shorter-spaced arrays also enables synthesis of a more ideal vertical response function with potentially higher vertical resolution. To better utilize the more complete data acquired by the array instruments, new interpretation technology has focused on effective methods to *invert* the data—that is, to obtain the formation conductivity distribution given the data acquired by the instrument. Until recently most of the effort was focused on an assumed axisymmetric distribution of conductivity. In spite of these advances in technology there remain, however, just as many enigmatic examples of uninterpretable log responses as there have always been. A major variation on the inversion theme was modeling software for use in deviated boreholes, typically drilled from platforms offshore. Otherwise these logs were uninterpretable. However,

Manuscript received by the Special Editor August 2000, revised manuscript received August 2001.
[1]University of Utah, Department of Geology and Geophysics, Salt Lake City, UT
[2]ExxonMobil Upstream Research Company, Houston, TX

problems with conductivity log interpretation in conventional vertically-drilled boreholes occurred infrequently enough so that mostly they could be ignored—and they were.

Horizontal wells changed everything.

However, it has taken some time for the industry to recognize this because the industry has been, simultaneously, learning the art of interpreting measurement-while-drilling (MWD) propagation instrument responses. Suffice it to say that the connection of the instrument responses to formation resistivities was not understood. Boundary effects curiously named "polarization" horns were known to induce resistivity responses not corresponding to any resistivity in a heterogeneous medium. But these were not the only observed anomalies. The beginning of real progress is marked by the study of MWD two-megahertz propagation resistivity responses in horizontal wells drilled in the Kuparuk field on Alaska's north slope. A study by Klein, Martin, and Allen (KMA; 1997) identified reservoir *anisotropy* as a major source of confusion. Basically, KMA discovered that in horizontal wells in hydrocarbon-bearing reservoirs at least two separate components of conductivity can influence instrument responses. They further discovered that the ratio of these conductivities could be positively enormous compared to what almost everyone thought possible—up to 100:1!

KMA suggested strongly that formations could have at least two conductivity values, a horizontal and a vertical conductivity (referred to as σ_h and σ_v) at the same point in the formation. An induction logging instrument apparent conductivity response σ_a could have any value $\sqrt{\sigma_h\,\sigma_v} \le \sigma_a \le \sigma_h$. To interpret σ_a further requires a knowledge of the angle the instrument axis makes with the z axis of the conductivity tensor $\hat{\sigma}$. With axial dipole instruments this requires the inference of formation dip and strike from other instruments.

A way to view the deficiencies of contemporary axial-dipole array instruments is to note that in fully anisotropic formations they sample at most only 1/3 (if the instrument is vertical) of the potential data space (i.e., of the three possible direct coupled magnetic field components, only one—H_{zz}—is sampled; the cross-coupled terms are all zero in this case), and at least sample only 1/6 (if the instrument is significantly tilted and rolled on its axis there are three direct-coupled and three cross-coupled field components). If the full data space were sampled, the complete conductivity tensor at a point could be inferred. A conductivity tensor thus determined would be the same regardless of the instrument's orientation with respect to the tensor, removing the anisotropy-induced ambiguity in instrument response. In order to sample the full data space a transmitter comprising three mutually orthogonal coils, and a similar receiver is required. There is now demand in the marketplace for the services of such instruments, and they have recently become commercially available (Kriegshäuser et al., 2000).

Interest in transverse coil induction logging instruments was evident in the Soviet Union before there was any discernible interest in the West (Eidman, 1970; Kaufman and Kaganskii, 1972; Tabarovskii et al., 1976). The work of Tabarovskii and several coauthors (1976, 1977, 1979) is concerned with analytical analysis of radially layered anisotropic media. Much later, Tabbagh and Giannakopoulou (1995) discuss the same problem but employ numerical methods to compute model log responses.

In this paper the low-frequency apparent resistivity responses of such a triaxial induction instrument are investigated. Figure 1 schematically illustrates the important features of the system. Three mutually orthogonal transmitter coils source corresponding magnetic dipoles, denoted by

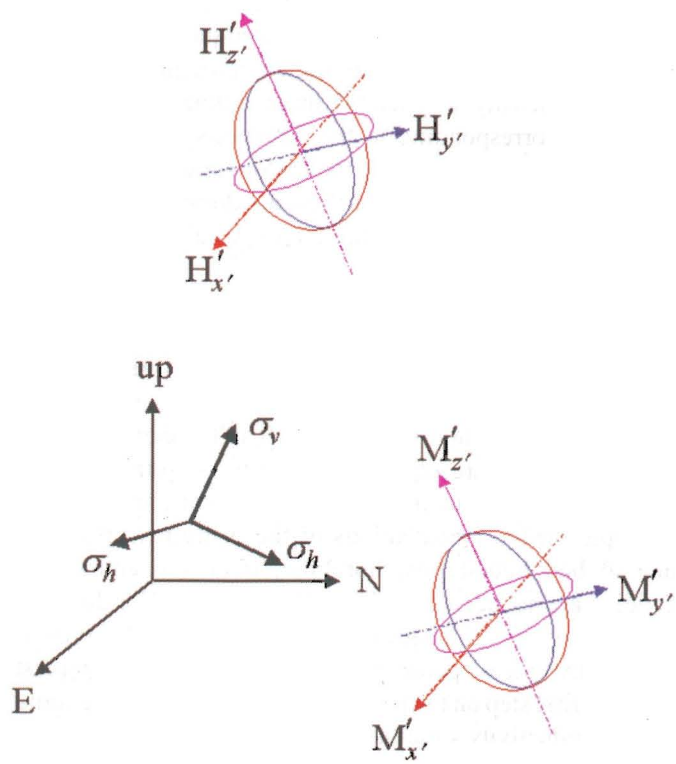

FIG. 1 Shown schematically are the transmitter and receiver arrays of a triaxial induction instrument. The coordinate system attached to the transmitter coils is called the instrument frame. The principal axes of a transversely isotropic conductivity tensor define another coordinate system called the medium frame. The x and y directions in this frame are freely chooseable since in the "horizontal" plane the conductivity is isotropic. Also shown is a coordinate frame attached to the earth (E,N,up) illustrating that neither the instrument nor the medium frames have any special directional relationship to the earth frame.

the **M**s. The total fields linking each corresponding receiver coil are denoted by the **H**s. The instrument axis and the conductivity tensor are each arbitrarily oriented with respect to coordinates fixed in the earth. Each of the three transmitters couples independently to each of the three receivers—thus from the nine magnetic field components nine components of apparent conductivity can be determined. Of the nine six are independent. These can be arranged in a 3×3 symmetric positive definite matrix. The three eigenvalues of this matrix comprise the three principal components of the conductivity. The principal components will be the same regardless of instrument orientation and regardless that the six independent components of the apparent conductivity matrix will in general depend on the orientation of the instrument coil system with respect to the principal components. The eigenvectors of the matrix will define the relative orientation of the instrument axes and the conductivity tensor principal axes. These might be useful to determine formation dip and strike (Moran and Gianzero, 1979).

Our method for estimating the components of the conductivity tensor is similar to the technique of Moran and Kunz (1962) for conventional induction logging. The magnetic flux density in each of three mutually orthogonal directions corresponding to the directions of the receiver axes is expanded in terms of its Taylor series. Terms linear in conductivity are retained as these are dominant at low frequency. The retained terms are then solved for an apparent conductivity.

The resulting conductivity expressions will apply, like that of Moran and Kunz, only to the simplest possible case. An anisotropic medium in which two of the three conductivity components are equal is termed transversely isotropic and is the simplest non-trivial case. (If all three of the principal components are equal the medium is isotropic.) Our results will apply in infinite, homogeneous, transversely isotropic media. Perturbations of the instrument response due to bed boundaries, borehole, invasion, and cross-bedding are not accounted for in this analysis. Nor does our analysis apply at frequencies corresponding to typical MWD instrument operation. Thus it represents the simplest possible first step on the road leading to a full understanding of the conductivity structure of a rock as derived from electromagnetic instrument responses observed in a borehole.

Our goal is to obtain estimates of the components of the conductivity tensor using voltages induced in each of three mutually orthogonal receiver coils of an induction logging instrument. These voltages are obtained from estimates of the magnetic flux linking each coil. The magnetic fields are easily computable from formulas only for sources located at the origin and directed along the coordinate axes of a coordinate frame, called the medium frame, chosen to coincide with the principal axes of the conductivity tensor. These formulas give the components of magnetic field in the same coordinate frame. In practice a borehole will penetrate the medium at an oblique angle with respect to this coordinate frame. A logging instrument in such a borehole would be coaxial with the borehole and rotated around the borehole axis by some unknown amount. Thus a coordinate frame attached to the instrument, called the instrument frame, with three mutually orthogonal axes aligned with the transmitter coil axes will not in general be aligned with the medium frame. In order to attain our goal we proceed beginning in the instrument frame, resolving each of the instrument's sources into their components in the medium frame, computing the components of field at the receiver locations in the medium frame using appropriate medium-frame formulas, and finally resolving each component of field into its three mutually orthogonal projections in the directions of the instrument frame coordinate axes. The sum of these projected components in the direction of each receiver dipole yields the resultant magnetic field linking each receiver coil. Finally, we show that at induction logging frequencies these magnetic field components are relatively simply related to the components of the conductivity tensor.

The formulas for the fields are obtained from procedures suggested by Moran and Gianzero (1979). We show that the transformations from the instrument-to-medium and back from the medium-to-instrument frames can be compactly expressed in tensor notation. Finally, our goal is reached in the development of low-frequency asymptotic expansions of the field expressions that simply relate the receiver voltages to the tensor components of formation conductivity. We will show that for a transversely isotropic medium the apparent conductivity tensor has only four independent components. Of these, only the component estimated from the axially oriented transmitter and receiver dipoles corresponds to the familiar induction instrument studied by Doll (1949) and Moran and Gianzero (1979). In addition to new results, we show how the previous work of Doll, Moran, and Gianzero can be obtained as a special case in our analysis.

MAGNETIC FIELD COMPONENTS

Medium coordinate frame representation

Consider a 3-D geoelectrical model of a homogeneous, unbounded, anisotropic medium with the tensor conductivity

$$\hat{\sigma} = \begin{bmatrix} \sigma_h & 0 & 0 \\ 0 & \sigma_h & 0 \\ 0 & 0 & \sigma_v \end{bmatrix}$$

where σ_h is the horizontal component of the conductivity and σ_v is the vertical component of the conductivity. We will confine ourselves to consideration of nonmagnetic media and, hence, assume that $\mu = \mu_0 = 4\pi \times 10^{-7}$H/m where μ_0 is the free-space magnetic permeability. The medium is excited through an electromagnetic field generated by magnetic dipoles with moment **M** and time dependence $e^{-i\omega t}$ where $\omega = 2\pi f$ and f is the natural frequency of the source. Displacement currents are neglected.

Maxwell's equations for the electromagnetic field are then

$$\nabla \times \mathbf{H} = \hat{\sigma} \cdot \mathbf{E} \tag{1}$$

$$\nabla \times \mathbf{E} = i\omega\mu_0 \mathbf{H} + i\omega\mu_0 \mathbf{M}\delta(x, y, z), \tag{2}$$

where $\delta(x, y, z)$ is a Dirac delta function located at the origin. Following Moran and Gianzero (1979) we can derive the expressions for the different components of the magnetic field generated by the induction transmitter dipoles aligned in each of the x, y, and z directions of the medium coordinate system. For each component of transmitter moment there are in general three components of induced field at each point in the medium. Thus there are nine formulas for field components. In this section we summarize these nine basic formulas for the magnetic field components.

A coordinate system with axes parallel to the principal axes of the conductivity tensor is convenient. Because in transversely isotropic media the conductivity tensor has two equal "horizontal" components, there is no preferred or unique choice of axes in the horizontal plane. Thus there is no loss of generality if the x–z plane is defined as the plane containing the σ_z principal axis and the borehole axis. The z axis is selected to coincide with the principal axis of $\hat{\sigma}$ which fixes the x axis as a line perpendicular to z lying in the x–z plane, with the direction of y axis (which is orthogonal to the x–z plane) determined by the right hand rule.

To proceed further we need to define a notation. The transmitter component is indicated by a superscript on the field symbol. Thus, $\mathbf{H}^x$ denotes the magnetic field generated by a point magnetic dipole at the origin horizontally oriented along the x axis having unit moment $\mathbf{M} = (1,0,0)$. Correspondingly, we denote as $\mathbf{H}^y$ the magnetic field generated by a point magnetic dipole horizontally oriented along the y axis having unit moment $\mathbf{M} = (0,1,0)$. Finally, the magnetic field generated by the vertically oriented point magnetic dipole having unit moment $\mathbf{M} = (0,0,1)$ is denoted as $\mathbf{H}^z$. In general, each component of the source induces three components of field in the medium. Components of field are indicated by subscripts. So $\mathbf{H}_i^j$ indicates the ith component of **H** due to the jth component of the transmitter, M_j; $i, j = x, y, z$.

Using the notation $\rho = \sqrt{x^2 + y^2}$, $s = \sqrt{\rho^2 + \lambda^2 z^2}$, $\lambda^2 = \sigma_h/\sigma_v$, $r = \sqrt{\rho^2 + z^2}$, $k_h^2 = i\omega\mu\sigma_h$, and $k_v^2 = i\omega\mu\sigma_v$ the expressions for the components of magnetic field per unit moment of source dipole are written as

$$H_x^x = \frac{e^{ik_v s}}{4\pi}\left[\frac{k_h^2}{\lambda s} + \frac{ik_h s - k_h k_v x^2}{s\rho^2} - \frac{2ik_h x^2}{\rho^4}\right] - \frac{e^{ik_h r}}{4\pi}\left[\frac{ik_h r - k_h^2 x^2}{r\rho^2} - \frac{2ik_h x^2}{\rho^4} - \frac{ik_h}{r^2} + \frac{k_h^2 x^2 + 1}{r^3} + \frac{3ik_h x^2}{r^4} - \frac{3x^2}{r^5}\right], \tag{3}$$

$$H_y^x = H_x^y = -xy\frac{e^{ik_v s}}{4\pi\rho^2}\left[\frac{k_v k_h}{s} + \frac{2ik_h}{\rho^2}\right] - xy\frac{e^{ik_h r}}{4\pi}\left[-\frac{k_h^2}{r\rho^2} - \frac{2ik_h}{\rho^4} + \frac{k_h^2}{r^3} + \frac{3ik_h}{r^4} - \frac{3}{r^5}\right], \tag{4}$$

$$H_z^x = H_x^z = -xz\frac{e^{ik_h r}}{4\pi}\left[\frac{k_h^2}{r^3} + \frac{3ik_h}{r^4} - \frac{3}{r^5}\right], \tag{5}$$

$$H_y^y = \frac{e^{ik_v s}}{4\pi}\left[\frac{k_h^2}{\lambda s} + \frac{ik_h s - k_h k_v y^2}{s\rho^2} - \frac{2ik_h y^2}{\rho^4}\right] - \frac{e^{ik_h r}}{4\pi}\left[\frac{ik_h r - k_h^2 y^2}{r\rho^2} - \frac{2ik_h y^2}{\rho^4} - \frac{ik_h}{r^2} + \frac{k_h^2 y^2 + 1}{r^3} + \frac{3ik_h y^2}{r^4} - \frac{3y^2}{r^5}\right], \tag{6}$$

$$H_z^y = H_y^z = -yz\frac{e^{ik_h r}}{4\pi}\left[\frac{k_h^2}{r^3} + \frac{3ik_h}{r^4} - \frac{3}{r^5}\right], \tag{7}$$

$$H_z^z = \frac{e^{ik_h r}}{4\pi r}\cdot\left[k_h^2 + \frac{ik_h}{r} - \frac{k_h^2 z^2 + 1}{r^2} - \frac{3ik_h z^2}{r^3} + \frac{3z^2}{r^4}\right]. \tag{8}$$

Since these component formulas assume unit-dipole sources, the field of a source of arbitrary magnitude is obtained by simply calculating the field using the formula and multiplying the result by the source magnitude.

Magnetic induction tensor

The magnetic field components are given in the previous section in a coordinate system defined by the horizontal and vertical principal axes of the transverse isotropic media. In practice, the orientation of the transmitter and receiver coils will be arbitrary (as well as a priori unknown) with respect to this coordinate system. Obviously, the instrument will respond only to flux from the field components linking the receiver coils. To proceed it is necessary to develop a connection between the magnetic field components detected by the instrument's receiver coils in a coordinate system defined by the coil axes (called $\mathbf{H}'$), and the components of the same field referred to the principal axes of the conductivity tensor (called $\mathbf{H}$) to which formulas (3)-to-(8) apply. In other words, a transformation of vectors—and tensors—from the instrument coordinate description to the

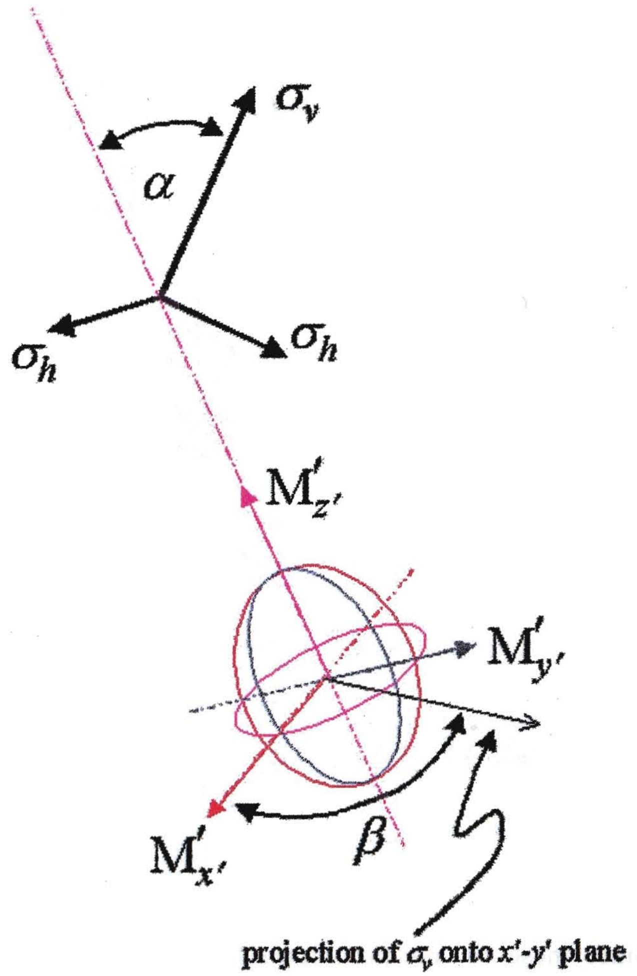

FIG. 2 If the direction of the σ_v principal axis of the conductivity tensor is (loosely) called the "vertical" axis, then the relative deviation angle α is measured between the vertical axis of the conductivity tensor and the instrument axis. The rotation angle β is the roll of the positive x-directed transmitter dipole around the instrument axis. The roll is measured from the highest intercept of a circle lying in the x-y plane centered on the instrument axis and the plane defined by the instrument axis and the vertical axis of the conductivity tensor to a point on the x-directed receiver axis.

medium coordinate description, and vice versa, is needed. Figure 1 shows schematically a sonde containing both three orthogonal transmitter coils with moments $\mathbf{M}^{x'}$, $\mathbf{M}^{y'}$, and $\mathbf{M}^{z'}$, and three orthogonal receiver coils oriented parallel to the transmitters. The instrument and medium axes are not parallel. Figure 1 also shows the relation of the axes x', y', z' of the instrument coordinates to the x, y, and z axes of the medium coordinates. The angle α between z and z' is a relative deviation of the instrument measured from the (not necessarily vertical) σ_z principal axis of the medium, and angle β is the roll, or relative rotation, that instrument's x'-directed transmitter dipole makes with the x–z plane (Figure 2). Formulas (3)-to-(8) represent the components of three vectors of magnetic fields in the tensor principal axes coordinate frame, each vector having three components. These three vectors form a magnetic tensor given in dyadic notation as

$$\hat{\mathbf{H}} = \mathbf{H}^x\,\mathbf{i} + \mathbf{H}^y\,\mathbf{j} + \mathbf{H}^z\,\mathbf{k}$$

where $\mathbf{i}$, $\mathbf{j}$, and $\mathbf{k}$ are the Cartesian basis vectors of the medium coordinates. We denote a tensor using a caret, or hat, over a bold type-faced variable symbol; vectors are similar, but hatless. Since $\mathbf{H}^x$ expands to $\mathbf{H}^x = H_x^x\mathbf{i} + H_y^x\mathbf{j} + H_z^x\mathbf{k}$ and similarly for the other vectors the dyadic function representation of the tensor in nonion form is

$$\begin{aligned}\hat{\mathbf{H}} = {} & H_x^x\,\mathbf{ii} + H_y^x\,\mathbf{ji} + H_z^x\,\mathbf{ki}\\ & + H_x^y\,\mathbf{ij} + H_y^y\,\mathbf{jj} + H_z^y\,\mathbf{kj}\\ & + H_x^z\,\mathbf{ik} + H_y^x\,\mathbf{jk} + H_z^z\,\mathbf{kk}.\end{aligned}$$

It is convenient to use the matrix representation of the dyadic function for which the coefficients of the dyads are written in a matrix as

$$\hat{\mathbf{H}} = \begin{bmatrix} H_x^x & H_x^y & H_x^z \\ H_y^x & H_y^y & H_y^z \\ H_z^x & H_z^y & H_z^z \end{bmatrix}.$$

The columns of this tensor are the magnetic field components in the medium coordinate frame for unit magnetic dipole transmitters in the directions of the basis vectors. For the magnetic field components of transmitters of arbitrary moment it is only necessary to multiply the appropriate column in the matrix by the actual moment of the transmitter in each direction. Multiplication of $\hat{\mathbf{H}}$ from the right by the column vector $\mathbf{M} = (M_x, M_y, M_z)^{\mathrm{T}}$ (where the superscript T denotes the transpose of a vector or matrix) accomplishes this. Now, since an arbitrarily oriented dipole of arbitrary moment can be resolved into its x, y, and z components, the usual interpretation of $\hat{\mathbf{H}}\mathbf{M} = \mathbf{H}$ is that $\mathbf{H}$ gives the components of the magnetic field at any point in space for a single transmitter dipole with components **M**. However, we consider here an alternative interpretation. It is clear from the derivation that $\hat{\mathbf{H}}$ can also represent the field of three physically separate, orthogonal, co-located dipoles (such as the triaxial transmitter of the tensor induction instrument that we are considering). The transmitters have a particularly simple representation in a coordinate frame with its origin co-located with the transmitter center and having basis vectors in the direction of the transmitter dipoles. This is referred to as the instrument frame. In the instrument frame we assume a source specified by $\mathbf{M}' = (1,1,1)$.

Instrument coordinate frame representation

In order to use our representation of the field tensor $\hat{\mathbf{H}}$ for an instrument located in an arbitrary orientation with respect to the tensor principal axes, it is necessary to transform between the transmitter moment (and other vectors) in the instrument coordinate frame representation (denoted (x',y',z')) into the medium frame representation (denoted by (x,y,z)).

The medium (unprimed) frame can be related to the instrument (primed) frame by two rotations about the origin (Figure 2). Let β measure the angle between the transverse transmitter axis designated x', and the line of intersection of the x'–y' plane with the x–z plane. Then, think of rolling the x'–y' plane around the z' axis through β until the x' transmitter (and receiver) lies in the x–z plane. We shall call this angle of rotation of the instrument on its axis the instrument roll, or relative rotation. Then a second rotation, of the z' axis, around the y' axis through an angle α until z' coincides with the medium axis z provides the desired transformation of coordinates. We shall call α the instrument tilt, or relative deviation.

The action of these rotations on a vector is mathematically represented by multiplication of vectors in the primed frame by rotation matrices. The rotation through β is represented by

$$\hat{\mathbf{R}}_\beta = \begin{bmatrix} \cos\beta & \sin\beta & 0 \\ -\sin\beta & \cos\beta & 0 \\ 0 & 0 & 1 \end{bmatrix}, \tag{9}$$

while the rotation through α is represented by

$$\hat{\mathbf{R}}_\alpha = \begin{bmatrix} \cos\alpha & 0 & -\sin\alpha \\ 0 & 1 & 0 \\ \sin\alpha & 0 & \cos\alpha \end{bmatrix}. \tag{10}$$

The matrix product $\hat{\mathbf{R}} = \hat{\mathbf{R}}_\alpha \hat{\mathbf{R}}_\beta$ gives the transformation of vector components from the instrument (primed) frame to the medium (unprimed) frame. This transformation, or rotation, matrix is (Moran and Gianzero, 1979)

$$\hat{\mathbf{R}} = \begin{bmatrix} \cos\alpha\cos\beta & \cos\alpha\sin\beta & -\sin\alpha \\ -\sin\beta & \cos\beta & 0 \\ \sin\alpha\cos\beta & \sin\alpha\sin\beta & \cos\alpha \end{bmatrix}. \tag{11}$$

As for any square matrix, $\hat{\mathbf{R}}\hat{\mathbf{R}}^{-1} = \hat{\mathbf{I}}$ where $\hat{\mathbf{I}}$ is the 3×3 identity matrix. The rotation matrices also have the special property that they are orthonormal. This means that their transposes are equal to their inverses; e.g., $\hat{\mathbf{R}}^{\mathrm{T}} = \hat{\mathbf{R}}^{-1}$.

Represented in the coordinates defined by the conductivity tensor principal axes the field is given in terms of its sources by

$$\mathbf{H} = \hat{\mathbf{H}}\mathbf{M}.$$

Denote the source moment by $\mathbf{M} = (M_x, M_y, M_z)^{\mathrm{T}}$ when referred to the medium frame and by $\mathbf{M}' = (M'_x, M'_y, M'_z)^{\mathrm{T}}$ when referred to the instrument frame. Let the coordinate rotation $\hat{\mathbf{R}}$ transform the magnetic field vector components from the instrument frame to the medium frame. For example, $\mathbf{H} = \hat{\mathbf{R}}\mathbf{H}'$ and $\mathbf{M} = \hat{\mathbf{R}}\mathbf{M}'$. Substituting $\mathbf{M} = \hat{\mathbf{R}}\mathbf{M}'$ into (12), multiplying from the left by $\hat{\mathbf{R}}^{-1}$, and defining $\mathbf{H}' \equiv \hat{\mathbf{R}}^{-1}\mathbf{H}$ gives

$$\mathbf{H}' = \hat{\mathbf{R}}^{-1}\hat{\mathbf{H}}\hat{\mathbf{R}}\mathbf{M}'. \tag{13}$$

This expresses the magnetic field in the instrument coordinate frame in terms of the source in the instrument coordinate frame and in terms of the magnetic induction tensor explicitly expressed in the medium coordinate frame. We note that with the definition

$$\hat{\mathbf{H}}' \equiv \hat{\mathbf{R}}^{-1}\hat{\mathbf{H}}\hat{\mathbf{R}} = \hat{\mathbf{R}}^{\mathrm{T}}\hat{\mathbf{H}}\hat{\mathbf{R}}, \tag{14}$$

that the field equations in the instrument frame have a form identical to their form in the medium frame; i.e.,

$$\mathbf{H}' = \hat{\mathbf{H}}'\mathbf{M}' \tag{15}$$

where $\hat{\mathbf{H}}'$ is the representation of the magnetic induction tensor in the instrument frame. The instrument's receiver voltages are proportional to the components of $\hat{\mathbf{H}}'$. For the unit dipole sources that we are discussing here, $\hat{\mathbf{H}}'$ can be thought of as the total instrument signal.

As a mathematical digression, it is interesting to note that while the vector transformation is given by, for example, $\mathbf{H} = \hat{\mathbf{R}}\mathbf{H}'$, the corresponding tensor transformation is given by $\hat{\mathbf{H}} = \hat{\mathbf{R}}\hat{\mathbf{H}}'\hat{\mathbf{R}}^{\mathrm{T}}$, having an additional factor of $\hat{\mathbf{R}}^{\mathrm{T}}$ on the right side of the $\hat{\mathbf{R}}\hat{\mathbf{H}}'$ product. The form of the tensor transformation is not intuitive, and cannot be inferred by analogy with the corresponding vector transformation. It is a mathematical formulation of the physical relationship between the magnetic moment in the transmitter and the magnetic field in the receiver. The tensor form shows that this relationship is independent of the choice of coordinate system.

APPARENT CONDUCTIVITY ESTIMATION

Basic instrument response

Induction logging instruments measure the voltages V induced in the receiver coils. For each coil

$$V = i\omega\mu_0 SH, \tag{16}$$

where S is the area of the receiver coil, and H is the magnetic field component along the axis of the coil. From the factor i in (16) it is seen that V is phase shifted 90° with respect to H. The magnetic field itself can be represented as a sum of the real ($\Re$), or in-phase, and imaginary ($\Im$), or quadrature, components decomposed as

$$H = \Re H + i\Im H. \tag{17}$$

Substituting (17) into (16), we obtain

$$V = -\omega\mu_0 S\,\Im H + i\omega\mu_0 S\,\Re H. \tag{18}$$

The magnetic field at the receiver comprises the sum of two fields, the so-called primary and secondary fields. The primary field is not part of the signal but represents the direct coupling of the transmitter to the receiver. This field is in-phase with the transmitter current. The voltage induced in the receiver by this field is in quadrature with the transmitter current. This primary field is rejected by the instrument. The electromotive force (emf) induced in the formation is also in quadrature with the transmitter current. This emf induces eddy currents in phase with itself. These eddy currents give rise to a secondary magnetic field that couples to the receiver coil, which responds with a voltage in quadrature with the eddy currents and secondary fields. This voltage is phase shifted –180° with respect to the transmitter current, but is still referred to as in-phase with the transmitter. This is the so-called R-signal (Moran and Kunz, 1962).

The in-phase component of the field (receiver voltage in quadrature or X-signal) is not easy to observe because of the much larger primary field. The quadrature component of the magnetic field (receiver voltage in phase, R-signal) is generated entirely by currents induced in the medium. In the conductivity range of sedimentary rocks and at induction logging frequencies the in-phase contribution of the secondary field caused by induced currents is much smaller than the quadrature component (Kaufman and Keller, 1989) and is not needed in estimating formation conductivity at low frequencies or conductivities. Therefore, the usual apparent conductivity definition is based on an approximate formula that considers only the imaginary (or quadrature) component of the induced magnetic field (i.e., in-phase receiver voltage). We will follow this principle here to derive expressions for the components of the apparent conductivity tensor.

Magnetic field asymptotic approximation

We obtain low frequency asymptotic approximations used in estimating apparent conductivity relations by expanding the exponential $e^{ik_v s}$ and $e^{ik_h r}$ in the form of Taylor series and substituting the resulting leading terms into formulas (3)–(8). (A detailed derivation of these approximate expressions is given in Appendix A.) The results are

$$\Im H_x^x \approx \frac{1}{4\pi}\omega\mu_0\sigma_h \left(\frac{y^2}{s\rho^2\lambda} + \frac{x^2}{r\rho^2} + 2x^2\frac{s-r\lambda}{\rho^4\lambda} + \frac{r\lambda - s}{\rho^2\lambda} + \frac{x^2}{2r^3} - \frac{1}{2r}\right), \tag{19}$$

$$\Im H_y^x = \Im H_x^y \approx \frac{xy}{4\pi}\omega\mu_0\sigma_h \left(2\frac{s-r\lambda}{\lambda\rho^4} - \frac{\lambda s - r}{\lambda r\rho^2 s} + \frac{1}{2r^3}\right), \tag{20}$$

$$\Im H_z^x = \Im H_x^z \approx \frac{xz}{8\pi r^3}\omega\mu_0\sigma_h, \tag{21}$$

$$\Im H_y^y \approx \frac{1}{4\pi}\omega\mu_0\sigma_h. \left(\frac{x^2}{s\rho^2\lambda} + \frac{y^2}{r\rho^2} + 2y^2\frac{s-r\lambda}{\rho^4\lambda} + \frac{r\lambda - s}{\rho^2\lambda} + \frac{y^2}{2r^3} - \frac{1}{2r}\right), \tag{22}$$

$$\Im H_z^y = \Im H_y^z \approx \frac{yz}{8\pi r^3}\omega\mu_0\sigma_h, \tag{23}$$

$$\Im H_z^z \approx \frac{r^2 + z^2}{8\pi r^3}\omega\mu_0\sigma_h. \tag{24}$$

The limiting case of these formulas for the instrument axis positioned parallel to the vertical axis of the conductivity tensor is interesting. In this limit for an instrument with transmitter-receiver spacing $z = L, \rho \to 0, \sigma \to \lambda L$, and $r \to L$. The quadrature components in this limit are

$$\Im H_x^x \approx \frac{\omega\mu_0}{8\pi L}\sigma_v, \tag{25}$$

$$\Im H_y^x = \Im H_x^y \approx 0, \tag{26}$$

$$\Im H_z^x = \Im H_x^z \approx 0, \tag{27}$$

$$\Im H_y^y \approx \frac{\omega\mu_0}{8\pi L}\sigma_v, \tag{28}$$

$$\Im H_z^y = \Im H_y^z \approx 0, \tag{29}$$

$$\Im H_z^z \approx \frac{\omega\mu_0}{4\pi L}\sigma_h. \tag{30}$$

Equation (30) indicates that for an instrument with its axis parallel to σ_v, the vertical magnetic field component of the vertical transmitter dipole is approximately proportional to the horizontal conductivity σ_h of the media. This is a well known result (Moran and Gianzero, 1979). Indeed, Doll's (1949) well known formula for the apparent resistivity of an axial dipole array corresponding to a vertically oriented instrument can easily be obtained from $\Im H_z^z$ using (18) with $S = \pi a_r^2$ where a_r is the receiver radius, and also remembering that the transmitter dipole in (30) is represented by a unit moment, $\mathbf{M}' = \mathbf{M} = (0,0,1) = (0, 0, I\pi a_t^2)$ where a_t is the transmitter radius. The result is

$$V = -\frac{(\omega\mu_0)^2\pi^2 a_t^2 a_r^2}{4\pi L}\sigma_h = -K\sigma_h \tag{31}$$

where K is Doll's instrument constant.

However, (25) and (28) indicate that the horizontal magnetic field components of the horizontal transmitter dipole are functions of the vertical conductivity only. This is a surprising result. It is counterintuitive based on the usual conceptual picture of the induction signal arising from eddy currents that, if circulating around a horizontal axis, would be influenced by both σ_h and σ_v. If confirmed in practice, this approximation would suggest the possibility of simply separating the horizontal and vertical effects in transverse isotropic media using a tensor system of observations.

EFFECTS OF SONDE ORIENTATION

Having derived low frequency asymptotic approximations for the field components in (19)–(24), we wish to inspect the accuracy of these approximations over a range of parameter values. We do this in the following sections by first developing a representation of the fields in polar coordinates in the x–z plane, and then applying this representation to an analysis of the accuracy of our approximation. We then examine the instrument response as a sonde at various tilt angles is rolled around its axis.

Tilt effects: relative deviation response

We have used Cartesian coordinates in the medium frame in equations (3)–(8), (19)–(24), and (25)–(30) to describe the magnetic fields. We have also shown how the rotation matrix given in (11) can be used to convert these expressions into the instrument frame. We now make this connection explicitly and derive formulas for the magnetic fields and the magnetic induction tensor expressed directly in the instrument frame.

The instrument's position is usually specified in terms of the angle between the instrument axis (obtained from a wellbore deviation survey) and the vertical direction. However, its response is conventionally described in terms of the relative deviation (denoted by α) which is the angle between the instrument axis and the direction normal to the (not necessarily horizontal) plane of isotropy in a transversely isotropic medium. This information could be available from borehole images or dipmeters, or might be inferred from structural maps. However, this information can be obtained directly from the tensor induction log data.

We shall show in the next section that the effect of sonde roll can be evaluated and eliminated from the observations. It is convenient for the present analysis to express **H** directly in terms of the relative deviation alone, with the relative rotation β taken as 0. Let the instrument's transmitter coils coincide with the coordinate origin, with the receiver coils located at some distance L from the transmitter at a point with polar coordinates in the x–z plane

$$x = L\sin\alpha, \quad y = 0, \quad z = L\cos\alpha, \tag{32}$$

where α is the relative deviation of the instrument axis with respect to the nominal vertical axis of the conductivity tensor. The x direction is chosen so that the instrument axis (i.e., L) is confined to the x–z plane, and the coil of the y-directed receiver is confined to the x–z plane. Therefore

$$\rho = x = L\sin\alpha,$$

$$s = \sqrt{\rho^2 + \lambda^2 z^2}, \quad = L\sqrt{\sin^2\alpha + \lambda^2\cos^2\alpha},$$

and

$$s - L\lambda = L\left(\sqrt{\sin^2\alpha + \lambda^2\cos^2\alpha} - \lambda\right).$$

With the restriction $\beta = 0$, using these formulas and equations (19)–(24), we obtain the following expressions for the magnetic field components at the various receivers as functions of α:

$$\Im H_x^x \approx \frac{\omega\mu_0\sigma_h}{4\pi L}\left[\frac{1+\sin^2\alpha}{2} + \frac{\sqrt{\sin^2\alpha + \lambda^2\cos^2\alpha} - \lambda}{\lambda\sin^2 a}\right];$$

$$\Im H_y^x = \Im H_x^y \approx 0;$$

$$\Im H_z^x = \Im H_x^z \approx \frac{\omega\mu_0\sigma_h}{8\pi L}\sin\alpha\cos\alpha;$$

$$\Im H_y^y \approx \frac{\omega\mu_0\sigma_h}{4\pi L}\left[\frac{1}{\lambda\sqrt{\sin^2\alpha+\lambda^2\cos^2\alpha}}-\frac{\sqrt{\sin^2\alpha+\lambda^2\cos^2\alpha}-\lambda}{\lambda\sin^2\alpha}-\frac{1}{2}\right];$$

$$\Im H_z^y = \Im H_y^z \approx 0;$$

$$\Im H_z^z \approx \frac{\omega\mu_0\sigma_h}{8\pi L}[1+\cos^2\alpha].$$

Summarizing these formulas in a matrix form, we have

$$\Im\hat{\mathbf{H}} = \begin{bmatrix} \Im H_x^x & \Im H_x^y & \Im H_x^z \\ \Im H_y^x & \Im H_y^y & \Im H_y^z \\ \Im H_z^x & \Im H_z^y & \Im H_z^z \end{bmatrix} \approx \frac{\omega\mu_0\sigma_h}{8\pi L}\cdot \tag{33}$$

$$\begin{bmatrix} 1+\sin^2\alpha + 2\dfrac{\sqrt{\sin^2\alpha+\lambda^2\cos^2\alpha}-\lambda}{\lambda\sin^2\alpha} & 0 & \sin\alpha\cos\alpha \\ 0 & 2\left[\dfrac{1}{\lambda\sqrt{\sin^2\alpha+\lambda^2\cos^2\alpha}} - \dfrac{\sqrt{\sin^2\alpha+\lambda^2\cos^2\alpha}-\lambda}{\lambda\sin^2\alpha}-\dfrac{1}{2}\right] & 0 \\ \sin\alpha\cos\alpha & 0 & 1+\cos^2\alpha \end{bmatrix}.$$

The off-diagonal 0s in (33) arise from the choice of coordinates and the choice of instrument orientation. In this representation the transverse transmitter and receiver dipoles are aligned parallel to the x and y axes when $\alpha = 0$. When $\alpha \neq 0$, the axis of the instrument lies in the x–z plane. However, the y-directed transmitter and receiver remain parallel to the medium frame y coordinate. Thus, with the confinement of the instrument axis to the x–z plane, and if the instrument cannot rotate on its longitudinal axis, no flux from the axial transmitter or the x-directed transmitter can link the y-directed receiver; this remains true regardless of the value of α. This also holds for the axial (or z-directed) component of transmitter and the y-directed transverse receiver. Put succinctly, the y-directed transmitter does not couple to the x- or z-directed receivers, nor does the y-directed receiver couple to the x- or z-directed transmitters. Consequently these terms are equal to zero in the induction tensor.

As in Cartesian coordinates, Doll's formula for the apparent resistivity can also be easily obtained from H_z^z in this form by letting $\alpha \to 0$. The term $1 + \cos^2\alpha = 2$ and making the same assumptions as before, formula (31) is again recovered.

Note that, although the induction tensor is now expressed in terms of the relative deviation α, the fields are still in the medium frame.

Figure 3 presents the results of a selected comparison between the exact analytical solutions for different magnetic field components computed by formulas (3)–(8), and their low frequency asymptotic approximations, calculated using formula (33). The results of field calculations are presented for a relative deviation angle α of the instrument $\alpha = 60°$. Other relative deviations show qualitatively similar responses. Nine plots are presented in the figure, corresponding to the nine magnetic field components calculated for different mutually orthogonal polarizations of the transmitter dipoles. The plots of these components are arranged in the form of a symmetric matrix reflecting the symmetry of the magnetic field components:

$$H_y^x = H_x^y = 0,\ H_z^x = H_x^z,\ H_y^z = H_z^y = 0.$$

In each component plot we show two curves: 1) an analytical solution (the solid line) for the quadrature magnetic field component, and 2) an asymptotic low frequency solution (circles) versus a dimensionless parameter ratio of the transmitter-receiver separation L to the horizontal skin depth $\delta_h = \sqrt{2/\omega\mu_0\sigma_h}$. One can see that, for a small L/δ_h ratio, these two curves practically coincide. They are approximately equal while L/δ_h is less than ≈ 0.01 and begin to diverge when $L/\delta_h > 0.05$ approximately. However, the approximation remains acceptable in most cases where L/δ_h is less than or equal to 0.1. Note that, for the typical induction logging instrument, the frequency is 20.0 kHz, and the distance between transmitter and receiver is equal to $L = 1.0$ m. The medium is characterized by $\sigma_h = 0.1$ S/m and $\sigma_v = 0.0625$ S/m, giving a coefficient of anisotropy $\lambda = 4$. For this case $L/\delta_h \approx 0.088$. For a well logging instrument having these parameters the low frequency asymptotic approximation provides a reasonable estimate of the actual magnetic field. Obviously the approximations are best for low frequencies and conductivities and become increasingly less accurate at higher frequencies and conductivities. This is just a manifestation of the long-familiar problem of skin effect that has been minimized in conventional instruments with a "skin effect boost."

Roll effects: relative rotation response

Figures 4–6 present the results of relative rotation response calculations. We calculated nine components of the matrix of the magnetic induction tensor in the instrument coordinate frame, using rotation formulas (14)

$$\hat{\mathbf{H}}' = \begin{bmatrix} H_{x'}^{x'} & H_{x'}^{y'} & H_{x'}^{z'} \\ H_{y'}^{x'} & H_{y'}^{y'} & H_{y'}^{z'} \\ H_{z'}^{x'} & H_{z'}^{y'} & H_{z'}^{z'} \end{bmatrix}.$$

The calculations were conducted for the following parameters: the horizontal conductivity was 0.1 S/m, the anisotropy coefficient was equal to $\lambda = 4$, the frequency was 20 kHz, and the distance between transmitter and receiver was equal to $L = 1$ m. We analyzed the induction tensor for; 1) a vertical borehole ($\alpha \approx 0°$); 2) a deviated borehole ($\alpha = 45°$); and 3) a horizontal borehole ($\alpha \approx 90°$). For every case we computed the tensor components as the relative rotation angle β varied from 0-to-360 degrees. We used the analytic formulas (3)–(8) and expression (14) to compute the rotation response. The results are shown in the form of polar diagrams of all nine components of the induction tensor. Figure 4 shows the polar diagrams of the imaginary components of an induction tensor for the vertical borehole. Figure 5 presents the same result for a deviated borehole with the relative deviation $\alpha = 45°$. Finally, Figure 6 presents the polar diagrams for the horizontal well. For convenience of observation, solid lines present the positive values of the magnetic field components, while the dashed lines show the negative values. The numbers at the upper right sides of each diagram are the scale factors. They represent the corresponding values of the solid circles that bound each diagram.

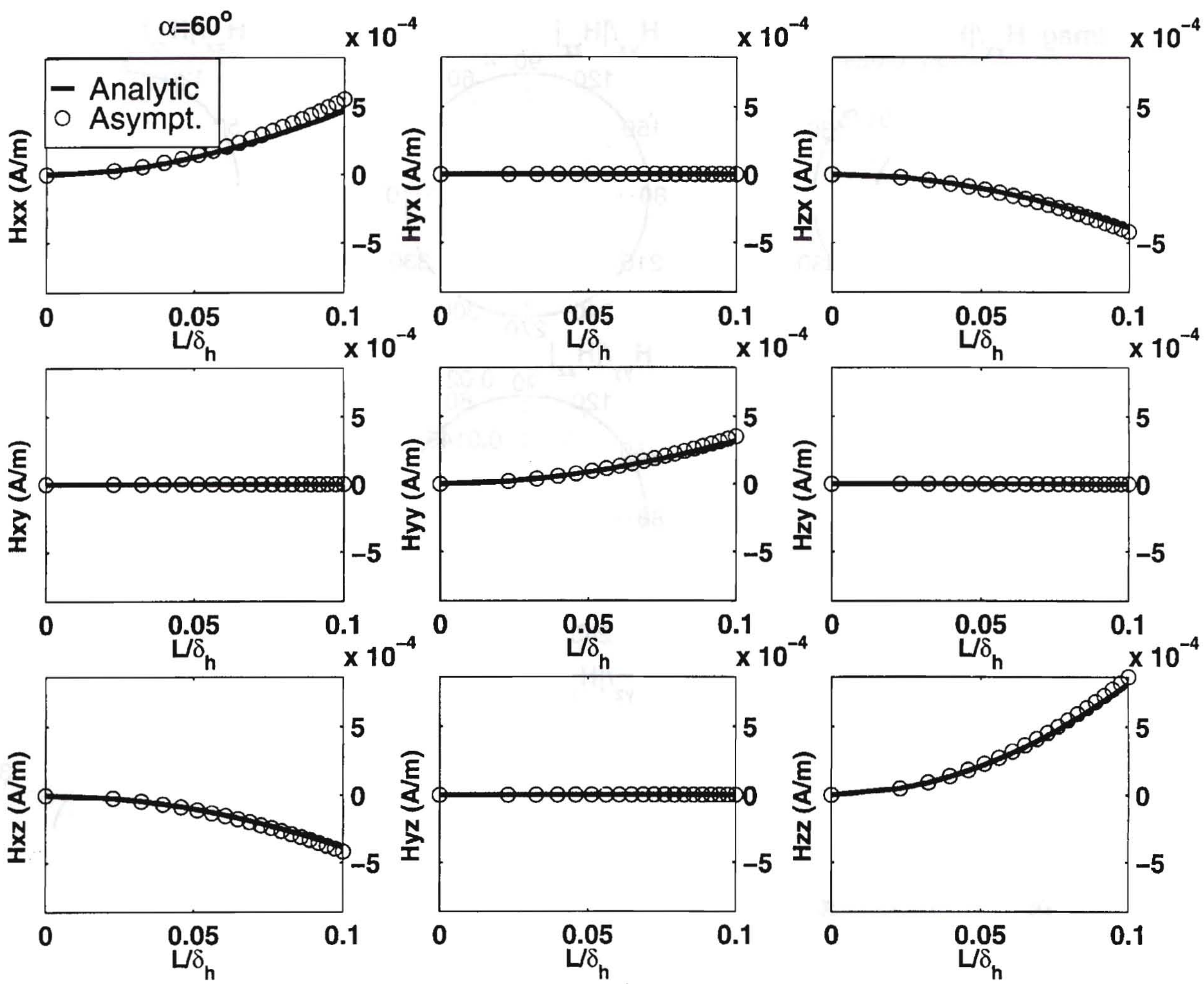

FIG. 3 Low frequency asymptotic (circles) and analytic solutions (lines) for the magnetic field in a homogeneous anisotropic medium for the deviation angle $\alpha = 60°$. The magnetic field components are plotted versus a dimensionless parameter ratio of the transmitter-receiver separation L to the horizontal skin depth $\delta_h = \sqrt{2/\omega\mu_0\sigma_h}$. For the typical induction logging instrument with $L = 1$ m, the interval $0 \le L/\delta_h \le 0.1$ corresponds to a frequency range from zero to ≈25.33 kHz ($1/4\pi^2 \times 10^6$), assuming $\sigma_h = 0.1$ S/m. The asymptotic solutions are used to estimate conventional (i.e., Doll) apparent resistivities but without correction for skin effect. At higher conductivities and frequencies the approximations become progressively less accurate.

Note that due to the symmetry of the induction tensor, the matrix of the polar diagrams is symmetrical with respect to the main diagonal. One can see in these plots that the polar diagram for component H_z^z is a circle, because this component doesn't depend on the relative rotation angle. All other polar diagrams have different but symmetrical shapes and vary for the different relative rotation angles of the well. Thus, the polar diagram representation makes it possible to describe the rotation effect in the induction tensor components. One can notice that, due to rotation, components of the induction tensor can change their signs, and even can be equal to zero for specific orientations. This circumstance should be taken into account in interpretation of the induction tensor well-logging results.

INSTRUMENT RESPONSE INTERPRETATION

In general it is not known a priori what values the conductivity components of a medium possess, or the direction of its principal axes with respect to the instrument. But there is enough information in the tensor induction instrument response to determine the values of α, β, σ_h, and σ_v. It is convenient to deconstruct the instrument signal beginning with a determination of β and the evaluation and elimination of its effects.

Analysis of roll effects: β determination

The instrument signal $\mathbf{H}'$ can be viewed as the components of a magnetic field expressed in the instrument coordinate frame. These components can be obtained from the

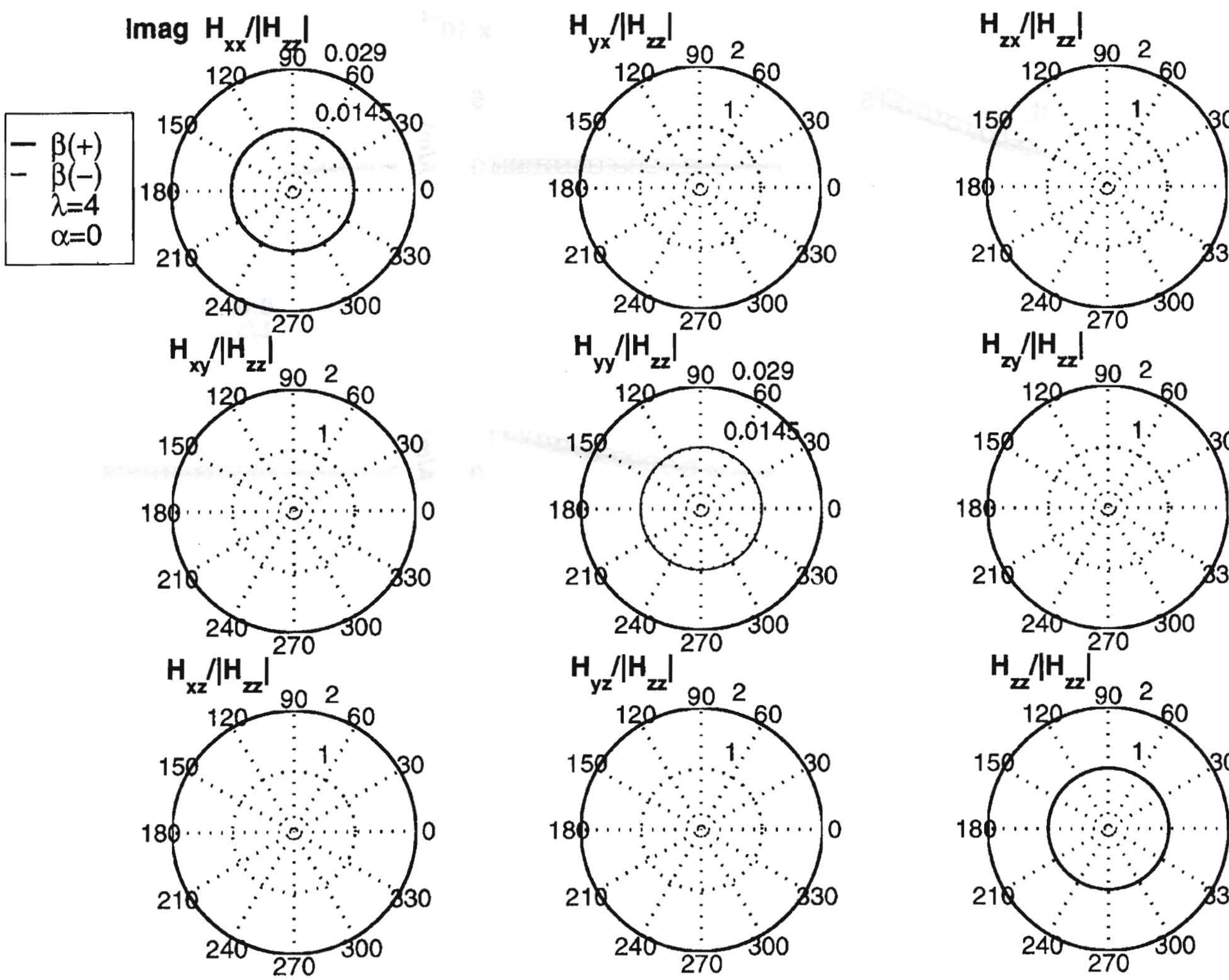

FIG. 4 Polar induction magnetic tensor diagram for the deviation angle $\alpha \approx 0$. The imaginary part of the magnetic field is normalized by the vertical magnetic field $|\Im H_{zz}|$. In this model the frequency is 20 kHz and the horizontal conductivity is 0.1 S/m, the anisotropy coefficient is 4, and the transmitter-receiver distance is $L = 1$ m. The tensor components are rotated around the borehole by changing the relative rotation angle $0° \leq \beta \leq 360°$. For the vertical position all the cross-coupled components are zero and all the direct-coupled components are constant regardless of the sonde rotation (i.e., roll).

same field expressed in the medium coordinates by a successive application of two coordinate rotations. This is expressed by equation (13). The magnetic induction tensor can be expressed in terms of the same rotation, as given in (14). Expanding (14) in terms of the component rotation matrices we see that

$$\hat{\mathbf{H}}' = \hat{\mathbf{R}}^{\mathrm{T}}\hat{\mathbf{H}}\hat{\mathbf{R}} = \hat{\mathbf{R}}_{\beta}^{\mathrm{T}}\hat{\mathbf{R}}_{\alpha}^{\mathrm{T}}\hat{\mathbf{H}}\hat{\mathbf{R}}_{\alpha}\hat{\mathbf{R}}_{\beta}\ . \tag{34}$$

$\hat{\mathbf{H}}'$ represents the instrument response in the instrument coordinate frame; i.e., each of its elements is the magnetic field at one of the receivers due to one of the transmitters. In general it will be fully populated. $\hat{\mathbf{H}}$ is the instrument response in medium frame, where the formulas for the fields have their simplest relation to the conductivity components of the medium.

From (34), clearly

$$\hat{\mathbf{R}}_{\beta}\hat{\mathbf{H}}'\hat{\mathbf{R}}_{\beta}^{\mathrm{T}} = \hat{\mathbf{R}}_{\alpha}^{\mathrm{T}}\hat{\mathbf{H}}\hat{\mathbf{R}}_{\alpha}\ . \tag{35}$$

The form of $\hat{\mathbf{R}}_{\beta}$ is known, but β is a priori unknown. We now show that the value of β can be obtained from the data. For convenience, we will temporarily introduce double primed variables to denote the matrix $\hat{\mathbf{H}}'' = \hat{\mathbf{R}}_{\alpha}^{\mathrm{T}}\hat{\mathbf{H}}\hat{\mathbf{R}}_{\alpha}$, and its elements. It turns out that all double primed variables can be eliminated in favor of the observations (i.e., single primed

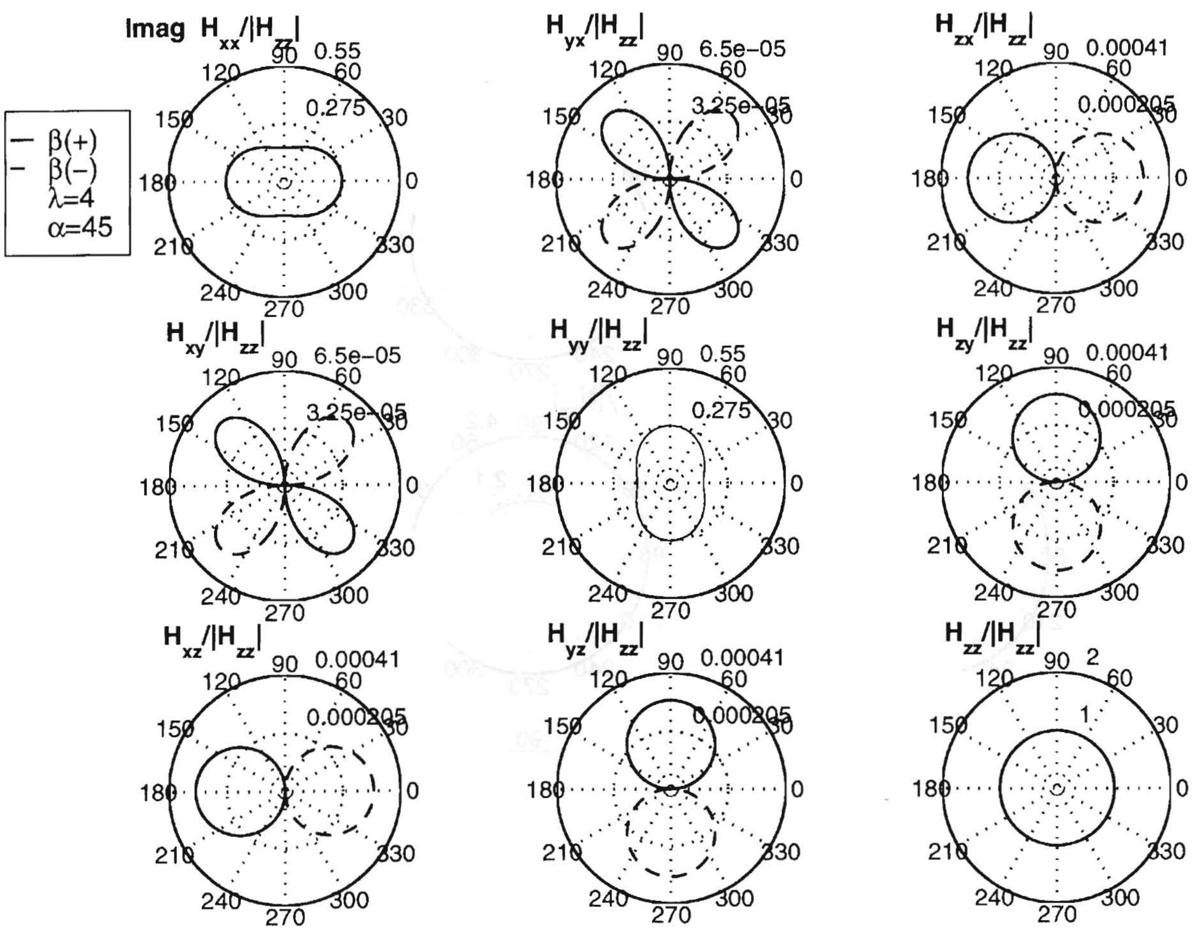

FIG. 5 The formation and instrument parameters are the same as those discussed in Figure 4. The relative deviation of 45° illustrates the interesting variation in the amplitude of the responses as a function of instrument roll. The H_{zz} component, corresponding to a conventional instrument, does not change, but all the others do. The H_{xx} and H_{yy} direct-coupled signals vary according to whether the transmitters and receiver coils lie in the vertical (or σ_z) plane or perpendicular to it. As the sonde rotates the H_{xx} and H_{yy} signals vary with the degree of roll. The cross-coupled terms vanish at orientations of the sonde where the magnetic field has mirror symmetry when viewed from the receiver coil, insuring that there can be no flux linkage and therefore no voltage induced. At other orientations the medium anisotropy breaks the symmetry and non-zero cross-coupled terms are induced. These change sign at the zero crossings, as indicated by the coding of the curves. Noting that H_{xx} and H_{xz} are phase shifted versions of H_{yy} and H_{yz}, having a constant phase lag of 90°, there are only four independent magnetic field components in transversely isotropic media.

variables). The observations are related to the sonde rotation by

$$\Im\hat{\mathbf{H}}' = \hat{\mathbf{R}}_{\beta}^{T}\, \Im\hat{\mathbf{H}}''\, \hat{\mathbf{R}}_{\beta}\,. \tag{36}$$

and thus

$$\Im\hat{\mathbf{H}}'' = \hat{\mathbf{R}}_{\beta}\, \Im\hat{\mathbf{H}}'\, \hat{\mathbf{R}}_{\beta}^{T}. \tag{37}$$

Multiplying out the factors on the right side and equating them term-by-term to the elements of the magnetic induction tensor (i.e., the instrument observations) produces equations for the observed field components in terms of β and the double-primed variables, from which the double-primed quantities can be eliminated. Expand (36) and equate the matrix elements on the left and right. Then from the matrix elements in the xx position

$$\Im H_{x'}^{x'} = \cos^{2}\beta\ \Im H_{x''}^{x''} + \sin^{2}\beta\ \Im H_{y''}^{y''}\,, \tag{38}$$

from the yy position

$$\Im H_{y'}^{y'} = \sin^{2}\beta\ \Im H_{x''}^{x''} + \cos^{2}\beta\ \Im H_{y''}^{y''}\,, \tag{39}$$

and from the xy and yx positions

$$\Im H_{x'}^{y'} + \Im H_{y'}^{x'} = \sin^{2}\beta\ (\Im H_{x''}^{x''} - \Im H_{y''}^{y''}). \tag{40}$$

Then subtracting (39) from (38) leads to

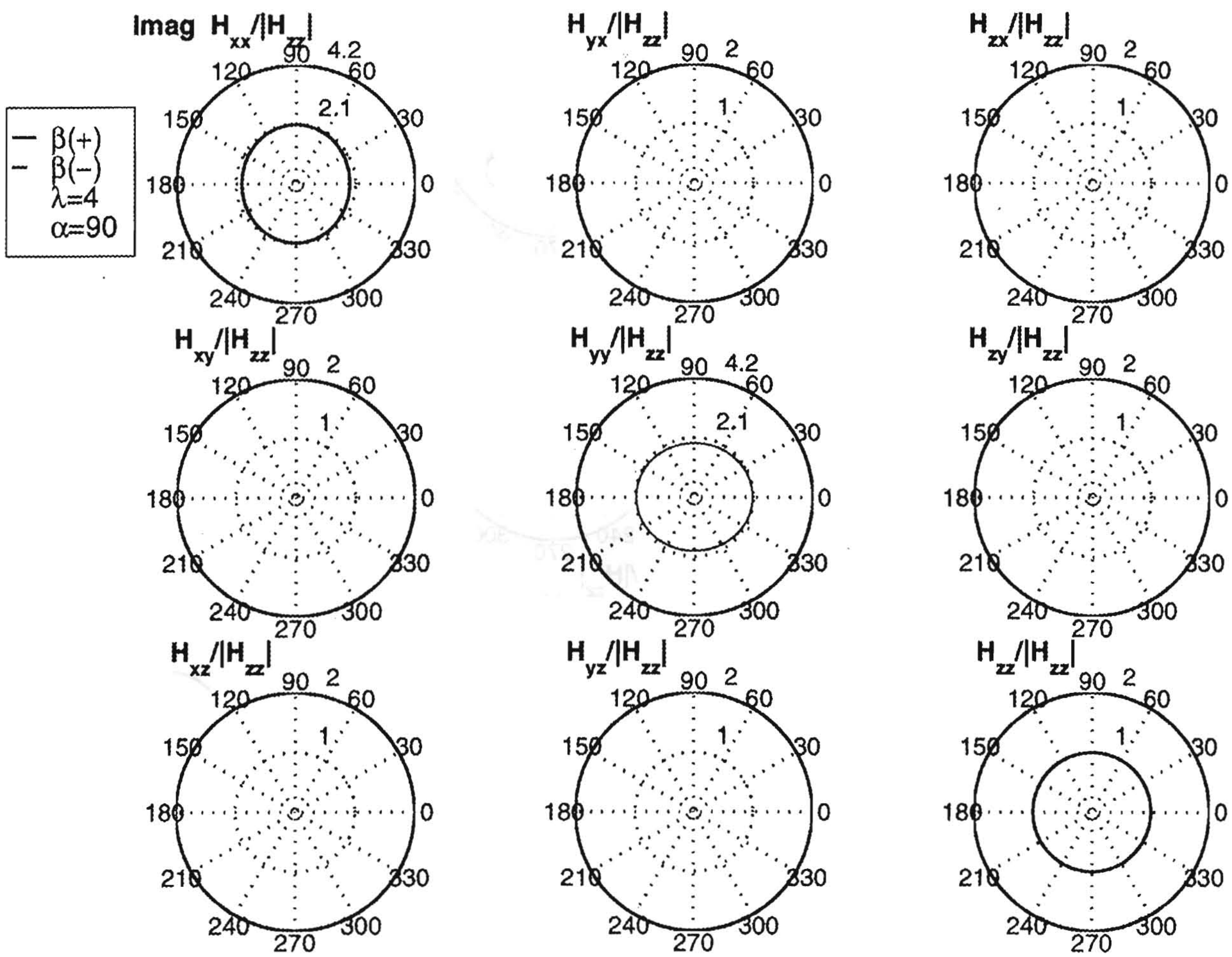

FIG. 6 The formation and instrument parameters are the same as those discussed in Figure 4. At the relative deviation of 90° the cross coupling terms again vanish for all values of instrument roll. This can be understood in terms of symmetry of the fields most easily by considering that a transverse dipole at any value of instrument roll can be considered to be the superposition of an appropriately weighted horizontal and vertical dipole. These components do not cross-couple and therefore the superposition of the components cannot cross couple either. The H_{xx} and H_{yy} direct-coupled signals vary in intensity according to whether the xx and yy arrays are parallel or perpendicular to the nominal horizontal plane.

$$\Im H_{x'}^{x'} - \Im H_{y'}^{y'} = (\cos^2\beta - \sin^2\beta)(\Im H_{x''}^{x''} - \Im H_{y''}^{y''}) \\ = \cos 2\beta(\Im H_{x''}^{x''} - \Im H_{y''}^{y''}) \,. \tag{41}$$

Then division of (40) by (41) permits the cancellation of the double-primed variables and gives the result

$$\tan 2\beta = \frac{\Im H_{y'}^{x'} + \Im H_{x'}^{y'}}{\Im H_{y'}^{y'} + \Im H_{x'}^{x'}}, \tag{42}$$

or, explicitly

$$\beta = \frac{1}{2}\tan^{-1}\left(\frac{\Im H_{y'}^{x'} + \Im H_{x'}^{y'}}{\Im H_{y'}^{y'} + \Im H_{x'}^{x'}}\right) \equiv \beta_a \,. \tag{43}$$

Note that β_a is expressed solely in terms of a subset of the observations, but it is not uniquely determined by the observations appearing in the formula. However, the quadrant which contains β_a is determined uniquely by the signs of $H_{z'}^{x'}$ and $H_{z'}^{y'}$, as shown in Table 1. Once β_a is known, the effects of sonde rotation on the observations can be removed using (35). The transformed observations depend only on α, σ_h, and σ_v. We shall call $\hat{\mathbf{R}}_\alpha^{\mathrm{T}}\Im\,\hat{\mathbf{H}}\hat{\mathbf{R}}_\alpha$ the "residual" signal.

Analysis of residual signal: σ_h, σ_v, and α determination

Consider again the case where the orientation of the instrument with respect to the principal axes of the medium is given by equations (32). Note that the axis z' of the instrument coordinates coincides with the instrument longitudinal axis. Since the instrument frame x' axis is confined to the medium frame x–z plane, the relative rotation β is 0 and the rotation matrix (11) takes the form

$$\hat{\mathbf{R}}_\alpha = \begin{bmatrix} \cos\alpha & 0 & -\sin\alpha \\ 0 & 1 & 0 \\ \sin\alpha & 0 & \cos\alpha \end{bmatrix}. \tag{10}$$

The instrument's signal, i.e., the quadrature component of the induction tensor, reduces in the instrument frame to

$$\Im\hat{\mathbf{H}}' = \hat{\mathbf{R}}_\alpha^{\mathrm{T}}\Im\hat{\mathbf{H}}\,\hat{\mathbf{R}}_\alpha \,, \tag{44}$$

where $\Im\hat{\mathbf{H}}$ is given by (33) and $\Im\hat{\mathbf{H}}'$ represents the instrument signal for the case $\beta = 0$. In Appendix B we describe a detailed derivation of the expression for the magnetic field components in the instrument system of coordinates. Based on this analysis we introduce a magnetic induction matrix for a sonde whose longitudinal axis makes an angle α with the σ_v axis of the conductivity tensor. If we define

$$q = \frac{\sqrt{\sin^2\alpha + \lambda^2\cos^2\alpha} - \lambda}{\lambda\sin^2\alpha}, \tag{45}$$

then using (33) and (44)

$$\Im\hat{\mathbf{H}}' = \begin{bmatrix} \Im H_{x'}^{x'} & \Im H_{x'}^{y'} & \Im H_{x'}^{z'} \\ \Im H_{y'}^{x'} & \Im H_{y'}^{y'} & \Im H_{y'}^{z'} \\ \Im H_{z'}^{x'} & \Im H_{z'}^{y'} & \Im H_{z'}^{z'} \end{bmatrix} \approx \frac{\omega\mu_0\sigma_h}{8\pi L} \tag{46}$$

$$\begin{bmatrix} 1 + 2q\cos^2\alpha & 0 & 2q\cos\alpha\sin\alpha \\ 0 & \left[\frac{2}{\lambda\sqrt{\sin^2\alpha + \lambda^2\cos^2\alpha}} - 2q - 1\right] & 0 \\ 2q\cos\alpha\sin\alpha & 0 & 2(1 + q\sin^2\alpha) \end{bmatrix}.$$

The instrument's response—i.e., the individual magnetic field components—are the matrix elements of (46):

$$\Im H_{x'}^{x'} = \frac{\omega\mu_0\sigma_h}{8\pi L}[1 + 2q\cos^2\alpha], \tag{47}$$

$$\Im H_{y'}^{y'} = \frac{\omega\mu_0\sigma_h}{8\pi L}\left[\frac{2}{\lambda\sqrt{\sin^2\alpha + \lambda^2\cos^2\alpha}} - 2q - 1\right],$$

$$\Im H_{z'}^{x'} = \frac{\omega\mu_0\sigma_h}{8\pi L}[2q\cos\alpha\sin\alpha] = \Im H_{x'}^{z'},$$

$$\Im H_{z'}^{z'} = \frac{\omega\mu_0\sigma_h}{8\pi L}[2 + 2q\sin^2\alpha]. \tag{48}$$

Note that (33) and (46) represent the *same* field. In (33), although the components are expressed in polar coordinates, they are still in the medium frame; in (46) they are in the instrument frame and represent the instrument signal.

Apparent conductivity: deviated instrument

The general case is for an instrument tilted with respect to the principal axes of the conductivity tensor and rolled by an arbitrary amount around the instrument axis.

For the axial dipoles the instrument roll is not a factor in the coupling of these dipoles to the medium or to each other. In this case assume that we use formula (48) to model measurements of $\Im H_{z'}^{z'}$ for a deviated instrument. Substituting for q in (48) and simplifying, the measured axial magnetic field is described by

$$\Im H_{z'}^{z'} = \frac{\omega\mu_0\sigma_h}{4\pi L}\frac{\sqrt{\sin^2\alpha + \lambda^2\cos^2\alpha}}{\lambda}. \tag{49}$$

Solving (49) for σ_h leads to

TABLE 1 Inspection of the signs of H_z^x and H_z^y determines the quadrant where β_a lies. The table was constructed by inspection of Figure 5.

H_z^y \ H_z^x	+	−
+	II	I
−	III	IV

$$\sigma'_{ha} = \frac{4\pi L}{\omega\mu_0}\Im H_{z'}^{z'} = \sqrt{\sigma_h^2\cos^2\alpha + \sigma_h\sigma_v\sin^2\alpha}\,. \quad (50)$$

Thus, for the axially directed transmitter and receiver corresponding to existing instruments, our formulation yields the formula of Moran and Gianzero (1979) for the apparent conductivity in a deviated borehole. With axial dipole instruments this formula is all that can be done. With the full data set of a triaxial instrument, the parameters of the medium can be solved for.

Equations (47) et seq. contain three unknown parameters: deviation angle α, horizontal conductivity σ_h, and vertical conductivity σ_v (disguised as the anisotropy coefficient $\lambda = \sqrt{\sigma_h\ \sigma_v}$). We can use these equations to find the parameters of the transverse isotropic media, and the deviation angle of the instrument from observed magnetic field components. For the special case of $\beta = 0$ lengthy but straightforward algebraic calculations presented in Appendix C provide direct analytical expressions for the solution. Let $g = \omega\mu_0/8\pi L$, then

$$\sigma_{ha} = \frac{1}{2g}\cdot \left[\Im H_{x'}^{x'} + \frac{1}{2}\Im H_{z'}^{z'} + \sqrt{\left(\Im H_{x'}^{x'} - \frac{1}{2}\Im H_{z'}^{z'}\right)^2 + 2\Im H_{z'}^{x'2}}\right], \quad (51)$$

$$\lambda^2 = \frac{4g^2\sigma_{ha}^2}{\Im H_{z'}^{z'}\left(\Im H_{x'}^{x'} + \Im H_{y'}^{y'} + \Im H_{z'}^{z'} - 2g\sigma_{ha}\right)}. \quad (52)$$

Of course, then

$$\sigma_{va} = \frac{1}{\lambda^2}\sigma_{ha} \quad (53)$$

and

$$\alpha_a = \frac{1}{2}\sin^{-1}\left[\frac{2\Im H_{z'}^{x'}}{\Im H_{x'}^{x'} + \Im H_{z'}^{z'} - 3g\sigma_{ha}}\right]. \quad (54)$$

In an infinite, homogeneous, transversely anisotropic medium these formation parameters would be exactly correct except for a skin effect reduction that we have not discussed. In heterogeneous media the same formulas are used, but the parameters are referred to as "apparent" conductivity, etc., signified by appending the a subscript *a*.

Apparent conductivity: vertical instrument

We have already presented results relating fields and conductivity components for a vertical instrument in formulas (25)–(30). These should represent the $\alpha \to 0$ limit for formulas (47) and (48). In this limit the results are

$$\Im H_x^x \approx \frac{\omega\mu_0}{8\pi L}\sigma_v\,, \quad (55)$$

$$\Im H_z^z \approx \frac{\omega\mu_0}{4\pi L}\sigma_h\,, \quad (56)$$

where primes are omitted for a vertical instrument. These are identical to (25) and (30) as expected. From the formula for the axial field quadrature component $\Im H_z^z$ for a vertical instrument, we obtain the expression for apparent conductivity

$$\sigma_a = \frac{4\pi L}{\omega\mu_0}\Im H_z^z \equiv \sigma_{ha}\,, \quad (57)$$

identical to Doll's expression.

Based on the formula for the transverse field quadrature component $\Im H_x^x$ for a vertical instrument, we obtain a new expression for apparent conductivity

$$\sigma_a = \frac{8\pi L}{\omega\mu_0}\Im H_x^x \equiv \sigma_{va}\,, \quad (58)$$

in agreement with the formulas derived for a vertical instrument; i.e., (25).

A final observation

We began our study with Moran's and Gianzero's (1979) formulation of the electromagnetic field response of a transversely isotropic medium. For completeness, we finish by observing that the determination of σ_{ha}, σ_{va}, α_a, and β_a permit the representation of an apparent conductivity tensor corresponding to *any* orientation of the instrument. This representation is $\hat{\sigma}'_a = \hat{\mathbf{R}}^{\mathrm{T}}\hat{\sigma}_a\hat{\mathbf{R}}$, where the subscripts indicate the "apparent" parameters. In the simple medium that corresponds to our analysis, the values of the "apparent" parameters will equal the values of the medium parameters, and the primed and unprimed variables indicate the instrument and medium frame respectively. The elements of $\hat{\sigma}$ are given in Moran and Gianzero (1979, p. 1284). We know that in general $\hat{\sigma}$ is symmetric, indicating that only six of its nine elements are independent. In the presence of transverse isotropy we might expect to see only four independent elements due to the additional symmetry of the medium. Moran and Gianzero show that in transversely isotropic media the six components of the conductivity tensor depend only on the four parameters σ_h, σ_v, α, and β. This makes explicit that regardless whether the representation is viewed from the medium frame (i.e., σ_h, σ_v, α, β) or is viewed from the instrument frame (i.e., σ_{xx}, etc.) only four parameters are required to specify the conductivity tensor.

NUMERICAL EXAMPLES: HOMOGENEOUS ANISOTROPIC MEDIUM

We have used formulas (51)–(54) and also formula (C.15) from Appendix C to calculate the apparent conductivities σ_{ha}, σ_{va}, apparent anisotropy coefficient λ_a, and relative deviation angle α_a on the basis of tensor well-logging data.

Calculations were conducted using $\sigma_h = 0.1$ S/m (10 Ω-m), $\sigma_v = \sigma_h/16 = 0.00625$ S/m (160 Ω-m). We precomputed the components of the induction tensor using the analytic formulas (3)–(8). We then applied (51)–(54) to the synthetic tensor induction log and generated plots of apparent conductivities σ_{ha}, σ_{va}, apparent anisotropy coefficient λ_a, and apparent deviation angle α_a versus a ratio of the transmitter-receiver separation L to the horizontal skin depth $\delta_h = \sqrt{2/\omega\mu_0\,\sigma_h}$. Solid lines in Figure 7 show the result of this calculation, i.e., the apparent conductivity, for an instrument with deviation $\alpha \approx 0°$, while the circles show the actual conductivity value of the tensor component (or other parameter). The apparent conductivity values are lower than the true conductivities. Figure 8 presents the same plot for $\alpha = 80°$. One can see in these plots that, in accordance with the theoretical formulas, the apparent parameters closely approach the true parameters of the model for low frequencies and conductivities and progressively diverge for higher frequencies; i.e., larger values of L/δ_h. Nevertheless, one can see that horizontal conductivity and the deviation angles are well approximated from the analytic tensor well log data in the interval $0 \le L/\delta_h \le 0.1$. The approximate vertical conductivity is less accurate, but the apparent vertical conductivity and apparent relative deviation are still approximately correct for the relative deviations up to and including 80°.

The deviation of the apparent conductivity from the formation conductivity is called "skin" effect in conventional induction logging, and is compensated by a so-called skin effect boost. The departure of the asymptotic approximations from the exact formation conductivity observed in Figures 7 and 8 is due to skin effect. If the method that we describe herein were to be used for actual interpretation, skin effect boosts would have to be developed for each component of apparent conductivity.

Our results suggest that determining the tensor conductivity components of a transversely isotropic medium from tensor induction observations in a deviated well is feasible if perturbations from a borehole and shoulder beds can be neglected, compensated, or corrected.

CONCLUSION

We have examined a simple but fundamental model of electromagnetic tensor induction well-logging in unbounded, homogeneous, transversely isotropic, conductive media using an arbitrarily oriented instrument. We have studied the analytical solution for induction tensor components and derived low frequency asymptotic approximations based on quadrature components.

The important result is that by measuring the quadrature components of the induction tensor we can obtain the principal values (i.e., σ_h and σ_v) and the orientation of the conductivity tensor with respect to the instrument. This conclusion holds whether the instrument is vertical, or rolled and tilted with respect to the tensor axes.

The formulas introduced above for the apparent horizontal and vertical conductivities σ_{ha}, σ_{va}, apparent anisotropy coefficient λ_a, and apparent deviation angle α_a, can be used as the basis for tensor well log interpretation in inhomogeneous anisotropic media when borehole and shoulder-bed effects can be neglected. This work strongly suggests that instruments developed using the triaxial induction principle will probably add great value to formation evaluation. However, corrections for borehole and shoulder-bed effects are sure to be required, if not in every case, then at least in many cases of practical interest.

The asymptotic formulas developed for the apparent conductivity are analogous to the Doll apparent resistivity formulas. Modern, practical interpretation of triaxial induction instrument responses will employ computational resources and methods not available to Doll. Our result completes Doll's classical method for all of the components of the magnetic induction tensor in a transversely isotropic medium and provides a bridge to the modern methods that will be based upon numerical models of the instrument responses.

The further development of principles for tensor induction interpretation in realistic cases is a topic of great interest with much work remaining to be done.

ACKNOWLEDGMENTS

The authors acknowledge the support of the University of Utah Consortium on Electromagnetic Modeling and Inversion (CEMI), which includes Advanced Power Technologies Inc., Baker Atlas Logging Services, BHP Minerals, EXXON Production Research Company, INCO Exploration, Japan National Oil Corporation, MINDECO, Mobil Oil Corporation, Naval Research Laboratory, Newmont Gold Company, Rio Tinto, Shell International Exploration and Production, Schlumberger-Doll Research, Unocal Geothermal Corporation, and Zonge Engineering.

We are thankful to Mobil for the partial support of Ertan Peksen.

REFERENCES

Doll, H. G., 1949, Introduction to induction logging and application to logging of wells drilled with oil base mud: *Journal of Petroleum Technology*, vol. 1, p. 148–162.

Eidman, I. E., 1970, Soviet patent 272448.

Kaufman, A. A. and Kaganskii, A. M., 1972, *Induction method of studying transverse resistance in boreholes* [in Russian], Nauka Press, Novosibirsk.

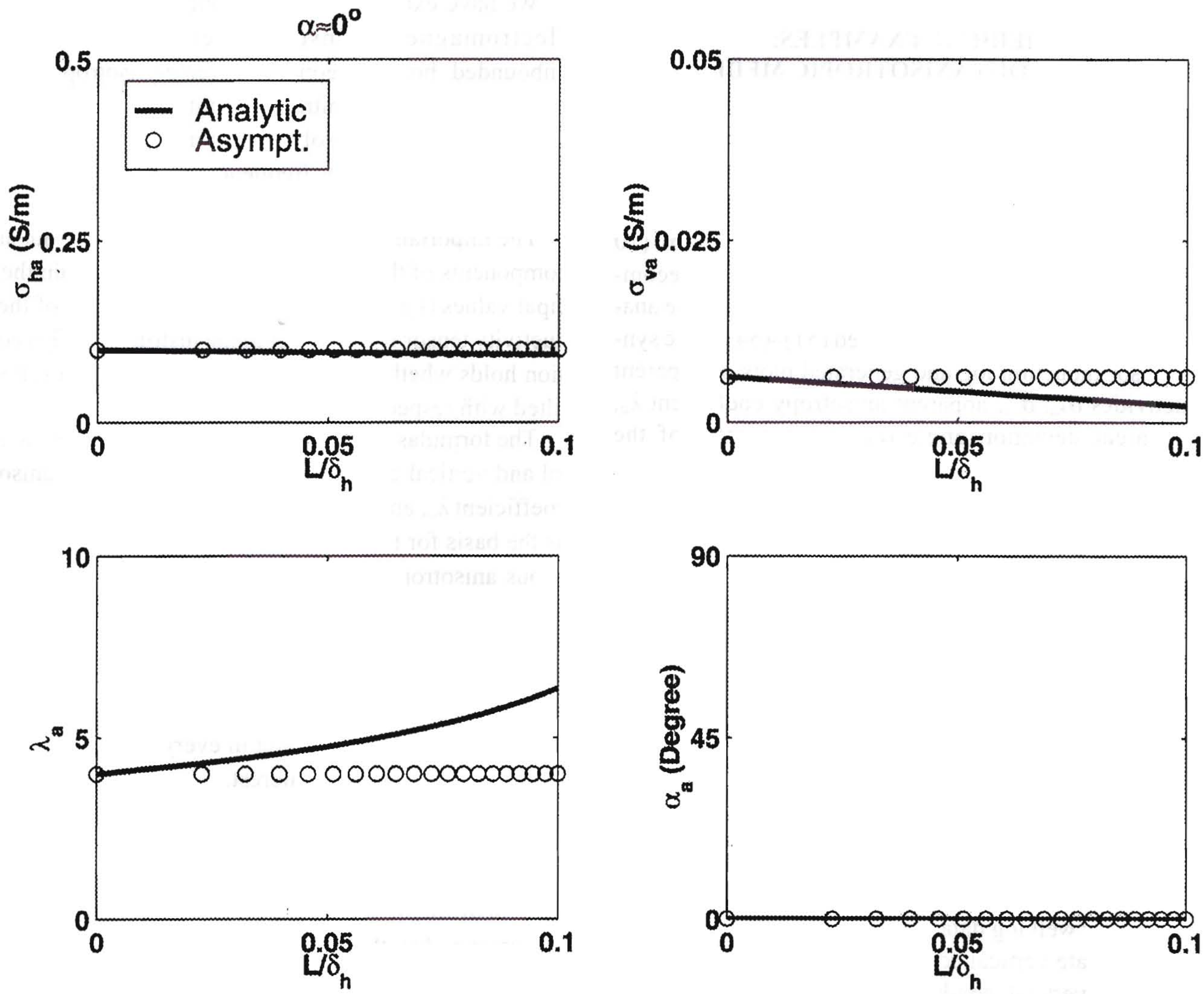

FIG. 7 True parameter values (circles) and apparent electrical conductivity parameters (lines) of a homogeneous anisotropic medium for the relative deviation angle $\alpha = 0°$. In the case of σ_h and σ_v these are the conventional apparent conductivities, but without correction for skin effect. At higher conductivities and frequencies the approximations become progressively less accurate. The parameters are plotted versus a dimensionless parameter ratio of the transmitter-receiver separation L to the horizontal skin depth $\delta_h = \sqrt{2 / \omega\mu_0\sigma_h}$. For the typical induction logging instrument with L = 1 m, the interval $0 \leq L/\delta_h \leq 0.1$ corresponds to a frequency range from zero to ≈25.33 kHz ($1/4\pi^2 \times 10^6$), assuming σ_h = 0.1 S/m.

Kaufman, A. A. and Keller, G. V., 1989, *Induction Logging*, Elsevier, Amsterdam, 597 pp.

Klein, J. D., Martin, P. R., and Allen, D. F., 1997, The petrophysics of electrically anisotropic reservoirs: *The Log Analyst*, vol. 33, no. 3, p. 25–36.

Kriegshäuser, B., Fanini, O., Forgang, S., Itskovich, G., Rabinovich, M., Tabarovsky, L., Yu, L., Epov, M., Gupta, P., and van der Horst, J., 2000, A new multicomponent induction logging tool to resolve anisotropic formations, paper D, *in* 41st Annual Logging Transactions: Society of Professional Well Log Analysts, 14 p.

Moran, J. H. and Kunz, K. S., 1962, The basic theory of induction logging and its application to two-coil sondes: *Geophysics*, vol. 27, no. 6, pp. 829–858.

Moran, J. H. and Gianzero, S. C., 1979, Effects of formation anisotropy on resistivity logging measurements: *Geophysics*, vol. 44, p. 1266–1286.

Tabarovskii, L. A., Kaganskii, A. M., and Epov, M. I., 1976, Electromagnetic field of a harmonic source in an anisotropic cylindrically layered medium: *Soviet Geology and Geophysics*, vol. 17, p. 74–79.

Tabarovskii, L. A., Epov, M. I., and Kaganskii, A. M., 1977, Focusing Systems of Induction Logging in Anisotropic Media: *Soviet Geology and Geophysics*, vol. 18, p. 81–87.

Tabarovskii, L. A. and Epov, M. I., 1979, Radial characteristics of induction focusing probes with transverse detectors in an anisotropic medium: *Soviet Geology and Geophysics*, vol. 20, p. 81–90.

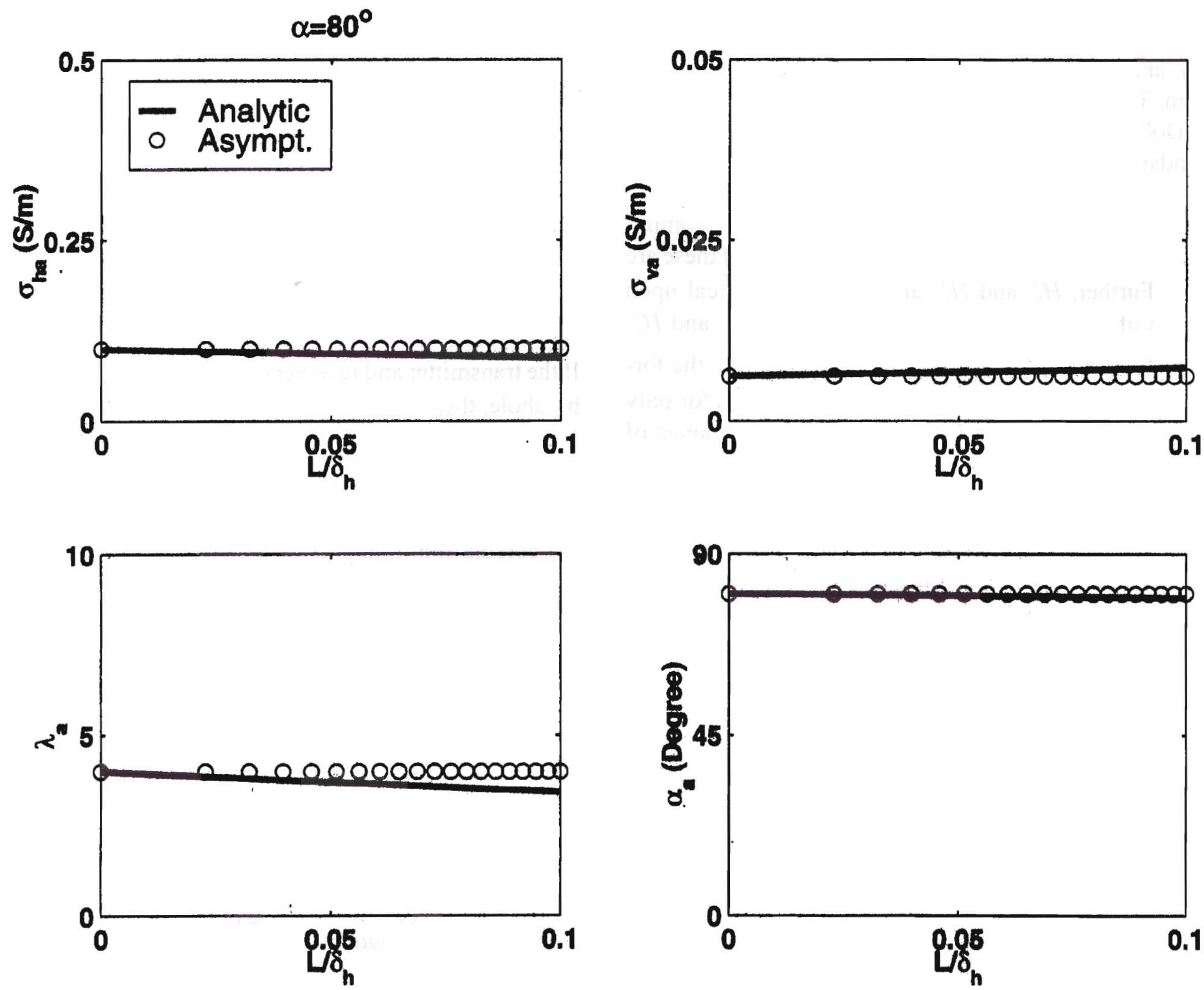

FIG. 8 True parameter values (circles) and apparent electrical conductivity parameters (lines) of a homogeneous anisotropic medium for the relative deviation angle $\alpha = 80°$. Except for the relative deviation, the model is the same as used in Figure 7. Obviously, the worst case for the asymptotic approximations is for very high relative deviations. Possibly a relative-deviation dependent skin effect boost could be found to mitigate this effect.

APPENDIX A: LOW FREQUENCY APPROXIMATION

The exponential terms, $e^{ik_v s}$ and $e^{ik_h r}$, appearing in the magnetic field formulas have Taylor series expansions given by

$$e^{ik_v s} = \sum_{n=0}^{\infty} \frac{(ik_v s)^n}{n!}, \quad e^{ik_h r} = \sum_{n=0}^{\infty} \frac{(ik_h r)^n}{n!}. \quad \text{(A.1)}$$

For low frequencies or conductivities these series can be approximated by their leading terms. Thus $e^{ik_v s} \approx 1 + ik_v s + \frac{1}{2} i^2 k_v^2 s^2$ and $e^{ik_h r} \approx 1 + ik_h r + \frac{1}{2} i^2 k_h^2 r^2$. These approximations are substituted into formulas (3)–(8) to obtain a closed-form low-frequency approximation of the magnetic field. The approximations are used to derive approximate formulas for the instrument responses linear in σ_h and σ_v. These formulas can be solved for approximations of the conductivities, σ_{ha} and σ_{va}, of an infinite, homogeneous, and anisotropic medium. The approximations are accurate to the same order as the Doll apparent conductivity formula that was the industry standard until recently—indeed the Doll formula is a special case contained in the formulas described below.

The magnetic induction tensor contains nine components, but since the tensor is symmetric, only six of these are distinct. Further, H_x^x and H_y^y are formally identical upon exchange of x and y in their respective formulas, and H_y^z can be obtained from H_x^z if x is replaced with y in the formula. In the interest of saving space the formulas for only four components are derived below, but upon exchange of appropriate variables (i.e., source and receiver labels) all nine components can be obtained from the four formulas given.

H^x field calculations

H_x^x **calculation**. The horizontal component of the magnetic field excited by the horizontal magnetic dipole is calculated by formula (3). Expanding the exponentials as outlined above and substituting the first three terms into (3), after much tedious algebra we obtain

$$H_x^x \approx \frac{1}{4\pi}\left[\frac{1}{s\rho^2\lambda}k_h^2\left(y^2 - s^2\left(1-2\frac{x^2}{\rho^2}\right)\right) + k_h^2\frac{x^2\rho^2 + r^2\rho^2 - 2r^2x^2}{r\rho^4} + k_h^2\frac{\left(\frac{1}{2}r^2 - \frac{1}{2}x^2\right)}{r^3} - \frac{r^2 - 3x^2}{r^5} + o(k_h^3 r^3)\right]. \quad \text{(A.2)}$$

The quadrature component is

$$\Im H_x^x \approx \frac{1}{4\pi}\omega\mu_0\sigma_h\left[\frac{1}{s\rho^2\lambda}\left(y^2 - s^2\left(1-2\frac{x^2}{\rho^2}\right)\right) + \frac{x^2\rho^2 + r^2\rho^2 - 2r^2x^2}{r\rho^4} + \frac{1}{2}\frac{x^2 - r^2}{r^3}\right]. \quad \text{(A.3)}$$

After some transformation

$$\Im H_x^x \approx \frac{1}{4\pi}\omega\mu_0\sigma_h \left[\frac{y^2}{s\rho^2\lambda} + \frac{x^2}{r\rho^2} + 2x^2\frac{s - r\lambda}{\rho^4\lambda} + \frac{r\lambda - s}{\rho^2\lambda} + \frac{x^2}{2r^3} - \frac{1}{2r}\right]. \quad \text{(A.4)}$$

If the transmitter and receiver coils are located in the vertical borehole, then $\rho \to 0$, $s \to \lambda|z|$, $r \to |z|$, and

$$\Im H_x^x \approx \frac{1}{8\pi}\omega\mu_0\sigma_v\frac{1}{|z|}. \quad \text{(A.5)}$$

H_y^x **calculation**. Using formulas (4) and the approximations based on (A.1) we obtain

$$H_y^x = \frac{xy}{4\pi}\left\{k_h^2\left[\frac{s}{\lambda\rho^4}\left(2 - \frac{\rho^2}{s^2}\right) + \frac{1}{r\rho^2} + \frac{1}{2r^3} - \frac{2r}{\rho^4}\right] + \frac{3}{r^5} + o(k_h^3 s^3)\right\}. \quad \text{(A.6)}$$

In this case the quadrature component is

$$\Im H_y^x \approx \frac{xy}{4\pi}\omega\mu_0\sigma_h\left[2\frac{s - r\lambda}{\lambda\rho^4} - \frac{\lambda s - r}{\lambda r\rho^2 s} + \frac{1}{2r^3}\right]. \quad \text{(A.7)}$$

For transmitter and receiver coils located in a vertical borehole, then $y \to 0$, $s \to \lambda|z|$, $r \to |z|$. The quadrature component is equal to

$$\Im H_y^x \approx \frac{xy}{4\pi\rho^2}\omega\mu_0\sigma_h\left[-2\frac{(\lambda^2-1)}{2\lambda^2|z|}-\frac{\lambda s-r}{\lambda rs}+\frac{\rho^2}{2r^3}\right]\to 0.$$

H_z^x **calculation**. Substituting the power series approximations into (5) we obtain

$$H_z^x = \frac{xz}{4\pi r^5}\left[3+\frac{1}{2}k_h^2 r^2 + o(k_h^3 r^3)\right]. \quad \text{(A.8)}$$

The quadrature component is

$$\Im H_z^x \approx \frac{xz}{8\pi r^3}\omega\mu_0\sigma_h. \quad \text{(A.9)}$$

For transmitter and receiver coils are located in a nearly vertical borehole $x \to 0, s \to \lambda|z|, r \to |z|$. In this case the quadrature component is equal to $\Im H_z^x \approx 0$.

H^y and H^z fields

The physical principle of reciprocity and the essential equivalence of the transverse source and receiver dipoles provides much redundancy in the formulas for the field components. Thus the formula for H_x^x is transformed into the formula for H_y^y when every y is replaced by an x, and every x is replaced by a y. By reciprocity H_x^y will equal H_y^x and the formulas will transform from one to the other upon exchange of xs and ys. The formula for H_z^y can be obtained by instrument symmetry from the formula for H_z^x when x is replaced with y. The formula for H_y^z is obtained by reciprocity from H_z^y upon exchange of y and z. So, by exploitation of these relations, only the H_z^z component remains to be calculated.

H_z^z **calculation**. The low frequency approximation for H_z^z is

$$H_z^z = \frac{1}{4\pi r^3}\left[\frac{3z^2-r^2}{r^2}+\frac{1}{2}k_h^2 r^2+\frac{1}{2}k_h^2 z^2 + o(k_h^3 r^3)\right]. \quad \text{(A.10)}$$

The quadrature component is

$$\Im H_z^z \approx \frac{r^2+z^2}{8\pi r^3}\omega\mu_0\sigma_h. \quad \text{(A.11)}$$

In a "vertical" borehole $x=0$ and $y=0$ then $\Im H_z^x \approx \omega\mu_0\sigma_h / 4\pi|z|$.

APPENDIX B: INDUCTION TENSOR IN THE INSTRUMENT COORDINATE FRAME

Consider a special case where the direction of the instrument axis with respect to the conductivity tensor axes is determined by the deviation angle α and the relative rotation angle β is equal to zero. We assume that three mutually orthogonal receiver coils are oriented along the instrument coordinate system x', y', z' and are located at the point (x, y, z) in the borehole at some distance L from the transmitter, according to formula (32). Note that the axis z' of the instrument coordinates coincides with the instrument longitudinal axis.

The rotation matrix (11) takes the form

$$\hat{\mathbf{R}}_\alpha = \begin{bmatrix}\cos\alpha & 0 & -\sin\alpha\\ 0 & 1 & 0\\ \sin\alpha & 0 & \cos\alpha\end{bmatrix} \quad (10)$$

The rotation formula (44) reduces to

$$\begin{bmatrix}H_{x'}^{x'} & H_{x'}^{y'} & H_{x'}^{z'}\\ H_{y'}^{x'} & H_{y'}^{y'} & H_{y'}^{z'}\\ H_{z'}^{x'} & H_{z'}^{y'} & H_{z'}^{z'}\end{bmatrix} = \quad \text{(B.1)}$$

$$\begin{bmatrix}\cos\alpha & 0 & -\sin\alpha\\ 0 & 1 & 0\\ \sin\alpha & 0 & \cos\alpha\end{bmatrix}\begin{bmatrix}H_x^x & H_x^y=0 & H_x^z\\ H_y^x=0 & H_y^y & H_y^z=0\\ H_z^x & H_z^y=0 & H_z^z\end{bmatrix}\begin{bmatrix}\cos\alpha & 0 & \sin\alpha\\ 0 & 1 & 0\\ -\sin\alpha & 0 & \cos\alpha\end{bmatrix} =$$

$$\begin{bmatrix}H_x^x\cos^2\alpha - 2H_z^x\sin\alpha\cos\alpha + H_z^z\sin^2\alpha & 0 & (H_x^x-H_z^z)\sin\alpha\cos\alpha + H_z^x(\cos^2\alpha-\sin^2\alpha)\\ 0 & H_y^y & 0\\ (H_x^x-H_z^z)\sin\alpha\cos\alpha + H_z^x(\cos^2\alpha-\sin^2\alpha) & 0 & H_x^x\sin^2\alpha + 2H_z^x\sin\alpha\cos\alpha + H_z^z\cos^2\alpha\end{bmatrix}$$

Using the last formula, we can find the expressions for all magnetic field components in the instrument coordinates. For later convenience in notation we define

$$q = \frac{\sqrt{\sin^2\alpha+\lambda^2\cos^2\alpha}-\lambda}{\lambda\sin^2\alpha} \quad \text{(B.2)}$$

$H_{x'}^{x'}$ **calculation**. Let us find $H_{x'}^{x'}$. The magnetic field components are equated to the corresponding components in (46).

$$\Im H_{x'}^{x'} = \Im H_x^x \cos^2\alpha - 2\Im H_z^x \sin\alpha\cos\alpha + \Im H_z^z \sin^2\alpha$$
$$= \frac{\omega\mu_0\sigma_h}{8\pi L}\left[1 + 2\cos^2\alpha\left(\frac{\sqrt{\sin^2\alpha + \lambda^2\cos^2\alpha} - \lambda}{\lambda\sin^2\alpha}\right)\right]$$
$$= \frac{\omega\mu_0\sigma_h}{8\pi L}[1 + 2q\cos^2\alpha]. \tag{B.3}$$

This component can also be expressed through vertical conductivity:

$$\Im H_{x'}^{x'} = \frac{\omega\mu_0\sigma_h}{8\pi L}\left[\lambda^2 + \frac{2\lambda\cos^2\alpha}{\sin^2\alpha}(\sqrt{\sin^2\alpha + \lambda^2\cos^2\alpha} - \lambda)\right]. \tag{B.4}$$

Thus,

$$\Im H_{x'}^{x'} = \Im H_x^x\left[\lambda^2 + \frac{2\lambda\cos^2\alpha}{\sin^2\alpha}(\sqrt{\sin^2\alpha + \lambda^2\cos^2\alpha} - \lambda)\right]. \tag{B.5}$$

On the other hand, for small α we have

$$\frac{\sqrt{\sin^2\alpha + \lambda^2\cos^2\alpha} - \lambda}{\sin^2\alpha} \approx \frac{1-\lambda^2}{2\lambda\cos\alpha}. \tag{B.6}$$

Therefore, for small α

$$\Im H_{x'}^{x'} = \frac{\omega\mu_0\sigma_v}{8\pi L}\left[(1-\cos\alpha)\lambda^2 + \cos\alpha\right]. \tag{B.7}$$

If $\alpha = 0$ then $\Im H_x^x = (\omega\mu_0 / 8\pi L)\sigma_v$. So for small α

$$\Im H_{x'}^{x'} = \Im H_x^x\left[(1-\cos\alpha)\lambda^2 + \cos\alpha\right]. \tag{B.8}$$

In the case of isotropic media $\lambda = 1$, and $\Im H_{x'}^{x'} = \Im H_x^x$.

$H_{z'}^{x'}$ **calculation**. Let us find $H_{z'}^{x'}$.

$$\Im H_{z'}^{x'} = (\Im H_x^x - \Im H_z^x)\sin\alpha\cos\alpha + \Im H_z^x(\cos^2\alpha - \sin^2\alpha)$$
$$= \frac{\omega\mu_0\sigma_h}{8\pi L}\left[2\cos\alpha\frac{\sqrt{\sin^2\alpha + \lambda^2\cos^2\alpha} - \lambda}{\lambda\sin\alpha}\right],$$
$$= \frac{\omega\mu_0\sigma_h}{8\pi L}[2q\cos\alpha\sin\alpha]. \tag{B.9}$$

In the case of isotropic media $\lambda = 1$, and $\Im H_{z'}^{x'} = \Im H_z^x = 0$.

$H_{y'}^{y'}$ **calculation**. Because of the choice of our coordinates $H_y^y = H_{y'}^{y'}$, and $H_{y'}^{y'}$ component doesn't change with the rotation. We have

$$H_{y'}^{y'} = \frac{\omega\mu_0\sigma_h}{8\pi r}\cdot$$
$$2\left[\frac{1}{\lambda\sqrt{\sin^2\alpha + \lambda^2\cos^2\alpha}} - \frac{\sqrt{\sin^2\alpha + \lambda^2\cos^2\alpha} - \lambda}{\lambda\sin^2\alpha} - \frac{1}{2}\right]$$
$$= 2\left[\frac{1}{\lambda\sqrt{\sin^2\alpha + \lambda^2\cos^2\alpha}} - q - \frac{1}{2}\right]. \tag{B.10}$$

$H_{z'}^{z'}$ **calculation**. For example, let us find $H_{z'}^{z'}$.

$$\Im H_{z'}^{z'} = \Im H_x^x \sin^2\alpha + 2\Im H_z^x\sin\alpha\cos\alpha + \Im H_z^z\sin^2\cos^2\alpha$$
$$= \frac{\omega\mu_0\sigma_h}{8\pi L}\left[-1 + \frac{2}{\lambda}\sqrt{\sin^2\alpha + \lambda^2\cos^2\alpha} + (\sin^2\alpha + \cos^2\alpha)^2\right]$$
$$= \frac{\omega\mu_0\sigma_h}{8\pi L}2[1 + q\sin^2\alpha]. \tag{B.11}$$

Thus,

$$\Im H_{z'}^{z'} = \frac{\omega\mu_0\sigma_h}{4\pi L}\frac{\sqrt{\sin^2\alpha + \lambda^2\cos^2\alpha}}{\lambda}. \tag{B.12}$$

If $\alpha = 0$,

$$\Im H_z^z = \frac{\omega\mu_0\sigma_h}{4\pi L}. \tag{B.13}$$

So

$$\Im H_{z'}^{z'} = \Im H_z^z\frac{\sqrt{\sin^2\alpha + \lambda^2\cos^2\alpha}}{\lambda}. \tag{B.14}$$

In the case of isotropic media $\lambda = 1$, and $\Im H_{z'}^{z'} = \Im H_z^z$. Summarizing the results in a matrix form, we have

$$\Im\mathbf{H}' \approx \frac{\omega\mu_0\sigma_h}{8\pi L}\cdot \tag{B.15}$$
$$\begin{bmatrix} 1 + 2q\cos^2\alpha & 0 & 2q\cos\alpha\sin\alpha \\ 0 & \left[\frac{2}{\lambda\sqrt{\sin^2\alpha + \lambda^2\cos^2\alpha}} - 2q - 1\right] & 0 \\ 2q\cos\alpha\sin\alpha & 0 & 2(1 + q\sin^2\alpha) \end{bmatrix}\begin{bmatrix} M_x \\ M_y \\ M_z \end{bmatrix}.$$

APPENDIX C: DERIVATION OF THE FORMULAS FOR APPARENT CONDUCTIVITIES AND THE ANISOTROPY COEFFICIENT

The derivation is based on the formula (46) for the induction matrix in the deviated borehole. Introducing the notations $g = \omega\mu_0/8\pi r$ and $\hat{\mathbf{h}}' = \Im\hat{\mathbf{H}}'/g\sigma_h$, and $q = (\sqrt{\sin^2\alpha + \lambda^2\cos a} - \lambda)/(\lambda\sin^2\alpha)$, for notational convenience, we make the definitions

$$h_{x'}^{x'} = 1 + 2q\cos^2\alpha \quad \text{(C.1)}$$

and

$$h_{y'}^{y'} = \frac{2}{\lambda\sqrt{\sin^2\alpha + \lambda^2\cos^2\alpha}} - 2q - 1 \quad \text{(C.2)}$$

$$h_{z'}^{x'} = h_{x'}^{z'} = 2q\cos\alpha\sin\alpha = q\sin 2\alpha \quad \text{(C.3)}$$

$$h_{z'}^{z'} = 2 + 2q\sin^2\alpha = 2(1 + q\sin^2\alpha). \quad \text{(C.4)}$$

Therefore $h_{x'}^{x'} + h_{z'}^{z'} = 3 + 2q$ and $h_{z'}^{x'} = q\sin 2\alpha$. Solving the last two equations, we obtain

$$q = \frac{1}{2}(h_{x'}^{x'} + h_{z'}^{z'} - 3) \text{ and } \sin 2\alpha = \frac{2h_{z'}^{x'}}{h_{x'}^{x'} + h_{z'}^{z'} - 3}. \quad \text{(C.5)}$$

On the other hand, obviously:

$$(h_{x'}^{x'} - 1)(h_{z'}^{z'} - 2) = h_{z'}^{x'2}. \quad \text{(C.6)}$$

Then, multiplying by $(g\sigma_h)^2$, we find

$$(\Im H_{z'}^{z'} - 2g\sigma_h)(\Im H_{x'}^{x'} - g\sigma_h) = \Im H_{z'}^{x'2} \quad \text{(C.7)}$$

and

$$2g^2\sigma_h^2 - g\sigma_h(2\Im H_{x'}^{x'} + \Im H_{z'}^{z'}) + (\Im H_{z'}^{z'}\Im H_{x'}^{x'} - \Im H_{z'}^{x'2}) = 0. \quad \text{(C.8)}$$

Expression (C.8) can be treated as the quadratic equation with respect to the unknown conductivity σ_h. Solving this equation, we find

$$\sigma_{1,2} = \frac{\Im H_{x'}^{x'} + \frac{1}{2}\Im H_{z'}^{z'} \pm \sqrt{(\Im H_{x'}^{x'} + \frac{1}{2}\Im H_{z'}^{z'})^2 + 2\Im H_{z'}^{x'2}}}{2g} \quad \text{(C.9)}$$

where $\sigma_{1,2}$ is simply intended to convey that the quadratic form has two possible solutions. For example, in the case of the vertical borehole

$$\Im H_x^x \approx \frac{1}{8\pi}\omega\mu_0\sigma_v\frac{1}{|z|} = g\sigma_v, \quad \text{(C.10)}$$

$$\Im H_z^z \approx \frac{1}{8\pi|z|^3}\omega\mu_0\sigma_h 2z^2 = \frac{1}{4\pi|z|}\omega\mu_0\sigma_h = 2g\sigma_h, \quad \text{(C.11)}$$

$$\Im H_z^x \approx 0. \quad \text{(C.12)}$$

Making these substitutions into (C.9) leads to

$$\sigma_{1,2} = \frac{\sigma_v + \sigma_h \pm |\sigma_v - \sigma_h|}{2}.$$

Taking into account that typically $\sigma_h > \sigma_v$, we obtain

$$\sigma_1 = \frac{\sigma_v + \sigma_h + |\sigma_v - \sigma_h|}{2} = \frac{\sigma_v + \sigma_h + (\sigma_h - \sigma_v)}{2} = \sigma_h.$$

and

$$\sigma_2 = \frac{\sigma_v + \sigma_h - |\sigma_v - \sigma_h|}{2} = \frac{\sigma_v + \sigma_h - (\sigma_h - \sigma_v)}{2} = \sigma_v.$$

It can be shown that in the general case of a deviated borehole

$$\sigma_1 = \sigma_h = \frac{\Im H_{x'}^{x'} + \frac{1}{2}\Im H_{z'}^{z'} + \sqrt{(\Im H_{x'}^{x'} - \frac{1}{2}\Im H_{z'}^{z'})^2 + 2\Im H_{z'}^{x'2}}}{2g}, \quad \text{(C.13)}$$

and

$$\sigma_2 = \frac{\Im H_{x'}^{x'} + \frac{1}{2}\Im H_{z'}^{z'} - \sqrt{(\Im H_{x'}^{x'} - \frac{1}{2}\Im H_{z'}^{z'})^2 + 2\Im H_{z'}^{x'2}}}{2g}$$

$$= \sigma_h\left[1 + \frac{\sqrt{\sin^2\alpha + \lambda^2\cos^2\alpha} - \lambda}{\lambda\sin^2\alpha}(2\cos^2\alpha + \sin^2\alpha)\right]. \quad \text{(C.14)}$$

In the case of small α

$$\sigma_2 \approx \sigma_h\left[1 + \frac{(1-\lambda^2)}{2\lambda^2\cos\alpha}(2\cos^2\alpha + \sin^2\alpha)\right] \approx \sigma_h\left[1 + \frac{(1-\lambda^2)}{\lambda^2}\right] = \frac{\sigma_h}{\lambda^2} = \sigma_v. \quad \text{(C.15)}$$

After determination of σ_h we can find α and q according to the formulas

$$q = \frac{1}{2}(h_{x'}^{x'} + h_{z'}^{z'} - 3) = \frac{1}{2g_0\sigma_h}(\Im H_{x'}^{x'} + \Im H_{z'}^{z'} - 3g\sigma_h),$$

and

$$\sin 2\alpha = \frac{2h_{z'}^{x'}}{h_{x'}^{x'} + h_{z'}^{z'} - 3} = \frac{2\Im H_{x'}^{z'}}{\Im H_{x'}^{x'} + \Im H_{z'}^{z'} - 3g\sigma_h}. \quad \text{(C.16)}$$

On the other hand

$$h_{y'}^{y'} = \frac{2}{\lambda\sqrt{\sin^2\alpha + \lambda^2\cos^2\alpha}} - 2q - 1. \quad \text{(C.17)}$$

Therefore,

$$q + \frac{1}{\sin^2 \alpha} = \frac{2}{\lambda^2 \sin^2 \alpha (h_{y'}^{y'} + 2q + 1)}. \quad \text{(C.18)}$$

From $h_{z'}^{z'} = 2 + 2q \sin^2 \alpha$ we have

$$\frac{1}{\sin^2 \alpha} = \frac{2q}{h_{z'}^{z'} - 2}. \quad \text{(C.19)}$$

Therefore,

$$q + \frac{1}{\sin^2 \alpha} = \frac{2}{\lambda^2 \sin^2 \alpha (h_{y'}^{y'} + 2q + 1)}. \quad \text{(C.20)}$$

Substituting (C.19) into (C.20), we obtain

$$\lambda^2 = \frac{4q}{h_{z'}^{z'} (h_{y'}^{y'} + 2q + 1)} = \frac{4}{h_{z'}^{z'} (h_{x'}^{x'} + h_{y'}^{y'} + h_{z'}^{z'} - 2)}. \quad \text{(C.21)}$$

Finally, replacing h_x^x with the corresponding H_x^x factor, etc., and substituting g where appropriate, we obtain the formula for the coefficient of anisotropy,

$$\lambda^2 = \frac{4g^2 \sigma_h^2}{\Im H_{z'}^{z'} (\Im H_{x'}^{x'} + \Im H_{y'}^{y'} + \Im H_{z'}^{z'} - 2g\sigma_h)}, \quad \text{(C.22)}$$

and

$$\sin 2\alpha = \frac{2\Im H_{z'}^{x'}}{\Im H_{x'}^{x'} + \Im H_{z'}^{z'} - 3g\sigma_h}. \quad \text{(C.23)}$$

ABOUT THE AUTHORS

Michael S. Zhdanov is Professor of Geophysics, Director of the Consortium for Electromagnetic Modeling and Inversion (CEMI). He received his MS in geophysics from Moscow Gubkin State University of Oil and Gas in 1968, MS in mathematics in 1969 and PhD in physics and mathematics in 1970 both from Moscow State University.

He was previously the Director of the Institute for Electromagnetic Research Studies, Moscow. Dr. Zhdanov is Honorary Gauss Professor, Gettingen Academy of Sciences, Germany, Full Member of Russian Academy of Natural Sciences, Honorary Professor of China National Center of Geological Exploration Technology.

His main research interest is developing methods for the solution of forward and inverse problems in geophysics, new techniques for electromagnetic imaging of the earth's interior. His approach includes theoretical study of model data and analysis of actual geophysical data, numerical modeling and inversion.

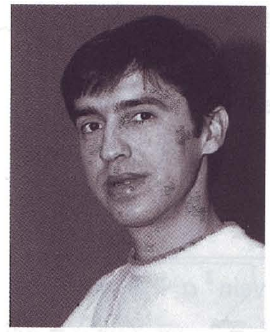

Ertan Peksen is a PhD student at the Consortium for Electromagnetic Modeling and Inversion (CEMI), the University of Utah. He graduated in 1993 (BS) from the University of Ankara, in geophysics. He received his Master of Science degree in geophysics from the Department of Geology and Geophysics, the University of Utah, in 1999. His research interest is modeling and inversion of tensor induction well logging in anisotropic media.

David Kennedy is currently a senior research associate at ExxonMobil Upstream Research Company. Prior to that there were 13 years at Mobil, both in research and operations services. His sojourn in the oil patch began in 1973 when Schlumberger was one of the few companies with the foresight to recruit newly-minted Georgia Tech physics graduates. After a five year stint with Schlumberger in the field in California and Alaska, and a brief flirtation with ARCO in Dallas, a full blown romance with graduate studies developed. David acquired MS degrees in Physics and Earth Sciences from the University of Texas at Dallas, but then jilted UTD for an infatuation with UC Berkeley, spending four fruitful years there but leaving without a PhD, jilted in his own turn. David has also worked briefly for Sohio and for Lockheed Missiles and Space Company. All this activity served an interest in acquiring, understanding, and interpreting borehole resistivity measurements. At Mobil David championed the use of resistivity modeling as a routine element of log interpretation. He has five patents and 17 publications and is internationally known as an expert in induction logging technology. He is Honorary Professor of Engineering at the Xi'an Petroleum Institute in Xi'an, China. David has had the pleasure of serving the industry since 1998 as editor of the well logging professional journal, *Petrophysics*. He resides in Sugar Land with his two darling children and his gracious and lovely mate.